Earth and Planetary Science Letters 359–360 (2012) 279–293

Contents lists available at SciVerse ScienceDirect

Earth and Planetary Science Letters

journal homepage: www.elsevier.com/locate/epsl

Lead and osmium isotopic constraints on the oceanic mantle from single abyssal peridotite sulfides

J.M. Warren [a,b,*], S.B. Shirey [a]

[a] Department of Terrestrial Magnetism, Carnegie Institution of Washington, 5241 Broad Branch Rd., NW, Washington, DC 20015, USA
[b] Department of Geological and Environmental Sciences, Stanford University, 450 Serra Mall, Stanford, CA 94305, USA

ARTICLE INFO

Article history:
Received 10 January 2012
Received in revised form
27 August 2012
Accepted 27 September 2012
Editor: T. Elliot
Available online 22 November 2012

Keywords:
abyssal peridotite
sulfide
Pb isotopes
Re–Os isotopes
mantle reservoirs

ABSTRACT

Single sulfides from abyssal peridotites have been analyzed for Pb and Re-Os to constrain the evolution of oceanic mantle composition. These represent the first analyses of Pb and Os isotopic compositions in the same sulfide grain. The sulfides are from Gakkel and Southwest Indian ridge peridotites, occur at $<0.1\%$ modal abundances, and contain 0.001–0.4 ppm Re, 0.003–5 ppm Os, and 0.12–12 ppm Pb. Sulfide Pb isotopic compositions extend from depleted (e.g., $^{206}Pb/^{204}Pb=17.0$) to enriched (19.6), covering a larger range than associated basalts. The Os isotopic range of sulfides is more restricted, but extends from depleted ($^{187}Os/^{188}Os=0.116$) to enriched (0.150). Pb and Os concentrations and isotopic compositions co-vary, with correlation coefficients of 0.76–0.94. Both Pb and Re–Os isotopic data follow ~ 2 Ga isochrons, with isotopic compositions varying down to small ($\ll 1$ km) length-scales and some sulfides containing supra-chondritic $^{187}Re/^{188}Os$ and $^{187}Os/^{188}Os$. These observations are best explained by long-term recycling of oceanic lithosphere combined with melt extraction and refertilization at ancient ocean ridges, rather than a specific event at 2 Ga.

The concentration of Pb in sulfides indicates that they host $<4\%$ of the mantle Pb budget. A re-evaluation of the mass balance of Pb in peridotites indicates that most mantle Pb is stored in silicate phases. The Pb partition coefficient between sulfide melt and silicate melt is estimated to be ~ 3, based on the correlation of Pb–Os concentrations in this study and measured Os partition coefficients from the literature. These observations indicate that sulfides do not exert a strong control on the fractionation of Pb during mantle melting, but they can be used to constrain mantle Pb isotopic composition.

Sulfides in this study, combined with literature data for Pb isotopes in peridotite whole rocks and pyroxene separates, provide evidence for ultra-depleted mantle, as 24% of peridotites are unradiogenic (i.e., $^{207}Pb/^{204}Pb<15.440$ and $^{206}Pb/^{204}Pb<17.726$), compared to only 3% of ridge basalts. This suggests that the mantle contains volumetrically significant reservoirs of ultra-depleted material, probably derived from recycled oceanic lithospheric mantle. These depleted reservoirs contribute in only small amounts to oceanic crust generation, both due to a limited ability to melt and to the dilution of any melt by more enriched melts during crust formation.

1. Introduction

The oceanic mantle has long been known to contain isotopic variations created by geologic processes much older than the 180 My age of the oldest ocean floor (e.g., Gast et al., 1964; Sun and Hanson, 1975; O'Nions et al., 1977). Among the most striking of the variations is the isotopic composition of Pb in young (<1 Ma) basalts from oceanic islands and ocean ridges, which fall along a correlated $^{207}Pb/^{204}Pb$–$^{206}Pb/^{204}Pb$ array that has a mean slope corresponding to a Pb–Pb age of $\sim 1.8-2$ Ga (e.g., Tatsumoto, 1966; Oversby and Gast, 1970; Sun, 1980; Chase, 1981). With such recently formed samples, this array clearly has no absolute age significance (Jacobsen and Wasserburg, 1979; Allègre et al., 1980; Hart, 1984; Albarède, 2001; Kellogg et al., 2007). Instead, it must record the integrated effects of a long history of mantle convection that may include prior ridge melting, the recycling of ancient oceanic crustal components, and the incorporation of ancient mantle domains residual after crust extraction and/or cratonization (e.g., Allègre, 1982; Zindler and Hart, 1986; Hofmann, 1997). An additional complication for Pb isotopes is that oceanic basalts are all enriched relative to the bulk composition of the Earth. Unradiogenic material has rarely been found in either oceanic or continental crustal

* Corresponding author at: Department of Geological and Environmental Sciences, Stanford University, 450 Serra Mall, Stanford, CA 94305, USA.
E-mail addresses: warrenj@stanford.edu (J.M. Warren), shirey@dtm.ciw.edu (S.B. Shirey).

0012-821X/$ - see front matter © 2012 Elsevier B.V. All rights reserved.
http://dx.doi.org/10.1016/j.epsl.2012.09.055

samples, with the absence of unradiogenic material giving rise to the "first Pb-paradox" (e.g., Allègre, 1969; Hofmann, 2003).

To understand the details of mantle compositional evolution, including the generation of depleted components, the full range of mantle enrichments and depletions must be documented. This is difficult in basalts, because depleted components are undersampled, both by being retained in more refractory components and by their lower concentrations in melts (Liu et al., 2008; Warren et al., 2009). In contrast, more isotopically enriched components dominate the isotopic signature of melts as these, by definition, have higher elemental concentrations. Recent studies of abyssal peridotites, which are the residues of ridge melting, have found extreme depletions in Nd, Os, Sr, and Hf isotopes that are not observed in basalts (Cipriani et al., 2004; Alard et al., 2005; Harvey et al., 2006; Liu et al., 2008; Warren et al., 2009; Stracke et al., 2011). However, analysis of Pb has remained difficult to accomplish in abyssal peridotites due to analytical difficulties associated with low concentration analyses (Warren et al., 2009). While <10 published Pb isotopic analyses exist for abyssal peridotites (Roden et al., 1984; Warren et al., 2009; Burton et al., 2012), thousands of isotopic analyses exist for Pb – and other radiogenically variable elements, such as Sr, Nd, and Hf – in oceanic basalts (e.g., Zindler et al., 1982; Hart, 1984; Hofmann, 1997; Meyzen et al., 2007).

In this study, Pb and Os isotopic compositions have been measured together, for the first time, in the same abyssal peridotite sulfide grains, with the express purpose of constraining the long term evolution of oceanic mantle composition. The affinity of Pb (a chalcophile element) and Os (siderophile) for sulfides results in different behavior for these two elements compared to lithophile elements, such as Sr, Nd, and Hf, which are all incompatible during melting and are hosted in silicates. The goal is to use the Re–Os and Pb radiogenic isotope systems to see through current ridge melting processes to look at much older mantle processes. In addition, the preservation of more depleted signatures in abyssal peridotites compared to basalts suggests that peridotites may preserve evidence for unradiogenic Pb that is rarely observed in melts. The ability to measure Pb and Os together in peridotite sulfides provides a technique to identify where unradiogenic material is stored in the Earth and to examine why Pb isotopes in oceanic basalts define correlated arrays.

Samples were selected from ultra-slow spreading segments of the Gakkel and Southwest Indian ridges, with the aim of analyzing depleted peridotites to look at residual mantle components. Fe–Ni–Cu sulfides are present in these peridotites at low ($<0.1\%$) modal abundances interspersed with silicate phases, as is typical in peridotites (e.g., Lorand, 1989a; Alard et al., 2000; Luguet et al., 2003). Ratios of $^{187}Os/^{188}Os$ are reported for 16 sulfides and Pb isotopic compositions for 12 sulfides, from 13 abyssal peridotites. These samples were picked as the most favorable for analysis out of 350 samples surveyed, based on sulfide abundance and grain size, combined with a low overall degree of sample alteration. Results indicate that sulfides contain less Pb than estimated in previous studies, but that they are powerful tracers for the compositional evolution of the mantle, particularly when combined with Os isotopes.

2. Geologic setting

On-axis sampling of abyssal peridotites in the past decade has improved the coverage of peridotites available for studying representative portions of the oceanic upper mantle, compared to earlier sampling that mainly focused on fracture zones. Axial peridotites are found at slow (<40 mm/yr full spreading rate) and ultra-slow (<20 mm/yr) spreading ridges, where normal faulting accommodates a large proportion of plate spreading. The overall degree of melting at these spreading rates is reduced due to on-axis conductive cooling (Cannat, 1993; Bown and White, 1994; Sleep and Barth, 1997; Dick et al., 2003; Montési and Behn, 2007). This results in short magmatic sections with focused melt extraction, separated by amagmatic sections where peridotite is emplaced directly on the axial seafloor by faulting (Dick et al., 2003; Cannat et al., 2006; Standish et al., 2008). Axial peridotites are thus the direct counterparts to MORBs collected from these ridges, while also representing the closest approximation to oceanic upper mantle composition due to limited degrees of melting.

Samples in this study are from the Gakkel Ridge (spreading rates of 6–15 mm/yr; Michael et al., 2003) and Southwest Indian Ridge (SWIR) Oblique Segment (spreading rates of 8–13 mm/yr; Standish et al., 2008). Selection of Gakkel and SWIR peridotites was based on the detailed petrographic analysis of 350 thin sections from these two ridges, which was done to identify samples with minimal degrees of alteration and with sufficient sulfide abundances for extraction. In addition, Gakkel peridotites were selected to provide representative geographic coverage along the ridge, though this was also constrained by variations in peridotite exposure as a function of the ridge segment tectonics (Michael et al., 2003). SWIR sampling focused on two Oblique Segment dredges, Van7-85 and Van7-96, as these have previously been studied for silicate Nd, Sr, and Pb isotopic compositions (Warren et al., 2009). Dredge Van7-85 consists of residual peridotites with depletions in light rare earth elements and low modal clinopyroxene, which make them typical of abyssal peridotites (e.g., Johnson et al., 1990). In contrast, dredge Van7-96 contains pyroxenite-veined peridotites that have silicate isotopic compositions indicative of interaction with Bouvet Hotspot, which passed near to the Oblique Segment around 15 Ma (Hartnady and le Roex, 1985).

Highly altered peridotites, defined as samples for which most or all silicate mineral phases are completely altered in petrographic thin sections, were excluded from this study. Peridotites in this study have $<50\%$ serpentinization, whereas most previous studies have used abyssal peridotites with $>50\%$ serpentinization (Luguet et al., 2003; Alt and Shanks, 2003; Bach et al., 2004; Alard et al., 2005; Harvey et al., 2006; Klein and Bach, 2009). Previous studies largely focused on two sections of the Mid-Atlantic Ridge (MAR): the Kane Fracture Zone and the Fifteen-Twenty Fracture Zone. Both of these regions have high degrees of alteration, typical of higher spreading rates, with samples in the study by Klein and Bach (2009) having 65–100% alteration. Both Alt and Shanks (2003) and Klein and Bach (2009) specifically focused on highly serpentinized samples to look at sulfide reaction pathways during hydrothermal alteration. In contrast, the Gakkel and SWIR samples are much fresher, as is typical of samples found at ultra-slow spreading rates. A few of the Gakkel samples are almost completely fresh, with $<5\%$ serpentinization and weathering.

3. Sulfide mineralogy

Peridotite sulfides can be divided into two groups: magmatic/mantle sulfides and hydrothermal sulfides (e.g., Lorand, 1989b; Alard et al., 2000; Luguet et al., 2003; Harvey et al., 2006). The magmatic/mantle sulfides are further subdivided into two groups: residual and metasomatic. Following the terminology of Lorand et al. (1999) and Luguet et al. (2001, 2003, 2004), "metasomatic sulfide" refers to any sulfide that has been reintroduced into the mantle by a percolating melt, whether by direct precipitation or by melt-rock reaction. In contrast, residual sulfides are grains that have survived partial melting, typically as inclusions within silicate

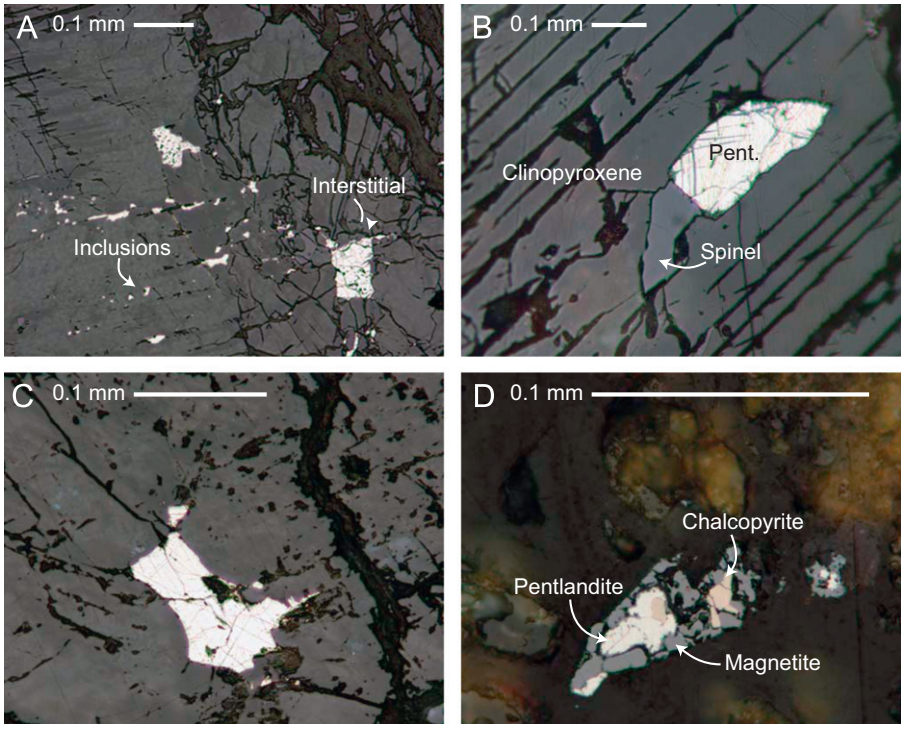

Fig. 1. Plane polarized reflected light photomicrographs of sulfides in abyssal peridotites. (A) Intergranular sulfides at boundary between olivine and pyroxene, and as inclusions in pyroxene (sample Vulc5-41-15). (B) Inclusion of pentlandite and spinel in clinopyroxene (sample HLY0102-34-24). (C) Intergranular sulfide displaying lobate grain boundaries with silicate matrix (sample Van7-86-28). (D) Two-phase intergranular sulfide, consisting of pentlandite and chalcopyrite, with alteration to magnetite (sample Van7-86-25).

minerals (Alard et al., 2000; Luguet et al., 2001; Harvey et al., 2006, 2011). Survival of partial melting implies a degree of melting $<10-15\%$ beneath the ridge axis, depending on the starting sulfur content of the peridotite (Luguet et al., 2003; Fonseca et al., 2012). Global estimates for degree of melting in abyssal peridotites and mid-ocean ridge basalts (MORBs) suggest an average of $<10\%$ melting (Klein and Langmuir, 1987; Johnson et al., 1990; Salters and Stracke, 2004; Workman and Hart, 2005), so preservation of residual sulfides in peridotites can occur. Detailed modeling of the SWIR Oblique Segment by Montési et al. (2011) indicates an average degree of melting of $\sim 7\%$, with a maximum of 12% for peridotites from this area.

The composition of residual and metasomatic sulfides plots in the Fe–Cu–Ni–S system, with minor Co and Zn (Dromgoole and Pasteris, 1987; Lorand, 1989b). At high temperature, the bulk composition of mantle sulfides corresponds to monosulfide solid solution (Mss) and intermediate solid solution (Iss). Subsolidus re-equilibration results in replacement of Mss by pentlandite–pyrrhotite and Iss by chalcopyrite (Kellerud et al., 1969; Lorand, 1989b; Alard et al., 2000). Luguet et al. (2003) found that mantle sulfides in abyssal peridotites consist mainly of pentlandite ($[Fe,Ni]_9S_8$), with additional occurrences of chalcopyrite ($CuFeS_2$) $\pm$ pyrrhotite (Fe_7S_8) $\pm$ bornite (Cu_5FeS_4).

Distinguishing between residual and metasomatic sulfides is based on mineralogical and textural relationships. Texturally, metasomatic sulfides are found in association with metasomatic minerals, such as amphibole, melt inclusions, and secondary clinopyroxene and spinels (Lorand, 1989b; Luguet et al., 2004; Alard et al., 2005). Luguet et al. (2001, 2003, 2004) found that pentlandites of metasomatic origin often have high Ni+Cu concentrations or that they occur in association with chalcopyrite and bornite, compositions that are similar to immiscible sulfides found in MORBs (Czamanske and Moore, 1977; Roy-Barman et al., 1998). At a bulk sample level, metasomatism is often associated with $Pd_N/Ir_N > 1$ (where N indicates normalization to chondrite), but heterogeneity among sulfide populations within individual samples means that each sulfide grain must be assessed individually to determine its origin (Luguet et al., 2001). Out of 13 peridotites in this study, eight were measured for bulk rock Pd and Ir concentrations (Warren, unpublished data). Only one sample, Van7-85-49, has $Pd_N/Ir_N > 1$, but petrographic observations indicate that all samples contain metasomatic sulfides.

Residual sulfides have predominantly pentlanditic compositions, suggesting an origin as refractory Mss grains, but the occurrence of pentlandite does not uniquely indicate a residual origin (Luguet et al., 2003). Residual sulfides tend to occur as inclusions within grains, which may allow them to survive high degrees of partial melting (Alard et al., 2000; Luguet et al., 2003; Harvey et al., 2006, 2011). However, the occurrence of a sulfide as an inclusion does not necessarily indicate a residual origin either. An example of a sulfide associated with metasomatic spinel, both of which are included in clinopyroxene, is shown in Fig. 1B. Detailed work by Luguet et al. (2001, 2003, 2004) has demonstrated that sulfide inclusions in clinopyroxene are often metasomatic, but that inclusions in orthopyroxene are generally of residual origin.

Alteration of peridotites by either seafloor weathering or serpentinization can result in partial replacement of mantle sulfides or direct precipitation of sulfides from hydrothermal fluids (Ramdohr, 1967; Lorand, 1985; Alt and Shanks, 2003; Luguet et al., 2003; Klein and Bach, 2009). Hydrothermal sulfides occur in veins or as disseminated grains and have a variety of compositions, including pentlandite, chalcopyrite, pyrrhotite, and occasionally pyrite and marcasite (Luguet et al., 2003, 2004). Weathering and serpentinization produce additional sulfide minerals (including magnetite, awaruite, godlevskite, heazlewoodite, millerite, polydymite, and native copper) as a function of low-temperature redox conditions (Luguet et al., 2003; Alt

Table 1
Abyssal peridotite sample descriptions and sulfide compositions.

Sample	Lith	Petrography	Grain	Wt (μg)	Os			$^{187}Os/^{188}Os$		Re			$^{187}Re/^{188}Os$		Pb				$^{208}Pb/^{204}Pb$		$^{207}Pb/^{204}Pb$		$^{206}Pb/^{204}Pb$		T_{MA}[b] (Ga)	T_{RD}[b] (Ga)
					pg	%Blank	ppm		2σ[a]	pg	%Blank	ppb		2σ[a]	pg	%Blank	ppm	2σ[a]		2σ[a]		2σ[a]		2σ[a]		
Gakkel, Eastern Volcanic Zone																										
HLY0102- 70-62	Harz	Sulf in Oliv/ Serp mesh	Sulf5	125	168	0.03%	1.35	0.1162	0.0004	38.7	0%	310	1.11	0.02	177	11%	1.41	0.03	36.956	0.129	15.335	0.040	17.034	0.115	−1.1	1.8
HLY0102-70-91	Lherz	Sulf in Oliv/ Serp mesh	Sulf1	4	9	0.60%	2.20			0.3	16%	82			15	60%	3.75	0.83	37.964	0.129	15.503	0.040	18.442	0.115		
Gakkel, Sparsely Magmatic Zone																										
HLY0102-04-43	Lherz	Interstitial Sulf	Sulf1	21	100	0.01%	4.74	0.1209	0.0004	5.1	8%	244	0.25	0.03											2.6	1.1
HLY0102-34-24	Lherz	Sulf enclosed in Cpx	Sulf1	5	6	0.13%	1.18	0.1267	0.0005																−0.1	0.7
PS59-201-39	Harz	Sulf in Oliv/ Serp mesh	Sulf1	68	14	0.38%	0.21	0.1238	0.0005	9.8	1%	144	3.36	0.15	37	38%	0.54	0.05	38.107	0.129	15.605	0.040	18.364	0.115	1.1	0.3
PS59-235-17	Lherz	Interstitial Sulf	Sulf5	17	81	0.07%	4.77	0.1267	0.0005	5.1	1%	301	0.30	0.02	73	23%	4.27	0.20	37.928	0.129	15.504	0.040	18.416	0.115	2.0	−0.5
PS59-317-6	Harz	Sulf in Opx	Sulf1	31	10	0.52%	0.33	0.1323	0.0005	1.1	5%	36	0.52	0.04	25	47%	0.79	0.11	38.197	0.129	15.599	0.040	18.610	0.115		
SWIR, Oblique Segment																										
PS86-6-38	Lherz	Large interstitial Sulf	Sulf1	116	236	0.00%	2.03	0.1500	0.0015	42.5	0.4%	367	0.87	0.01	1026	2%	8.85	0.04	37.937	0.095	15.575	0.032	18.534	0.092	2.8	−3.0
Van7-85-42	Lherz	Interstitial Sulf	Sulf1	285	122	0.01%	0.43	0.1278	0.0005	13.3	3%	47	0.53	0.01											−0.7	0.2
Van7-85-42	Lherz	Interstitial Sulf	Sulf2	47	36	0.02%	0.77	0.1274	0.0005	1.8	19%	38	0.24	0.01											0.5	0.2
Van7-85-47	Lherz	Interstitial Sulf	Sulf2	117	328	0.00%	2.82	0.1275	0.0005	31.6	1%	271	0.46	0.00											−2.5	0.2
Van7-85-47	Lherz	Sulf on Cpx cleavage	Sulf6	15	24	0.27%	1.60	0.1301	0.0011	1.0	6%	66	0.20	0.01	105	19%	6.99	0.36	38.081	0.084	15.624	0.026	18.384	0.114	−0.3	−0.2
Van7-85-47	Lherz	Sulf on Cpx cleavage	Sulf7	3						1.0	6%	337														
Van7-85-49	Lherz	Sulf on edge & inside Cpx	Sulf3	12	41	0.16%	3.40			1.6	4%	137			12	68%	0.99	0.45								
Van7-85-49	Lherz	Sulf on edge & inside Cpx	Sulf4	5						0.8	7%	168			29	46%	5.79	1.08	37.960	0.084	15.512	0.026	18.535	0.114		
Van7-85-49	Lherz	Sulf on Cpx cleavage	Sulf5	112	0.5	12.63%	0.004	0.1176	0.0023	0.3	17%	3	2.15	0.44	14	64%	0.12	0.05							−0.4	1.6
Van7-85-49	Lherz	Sulf in Oliv/ Serp mesh	Sulf6	91	0.3	19.69	0.003	0.1362	0.0031	0.1	38%	1	1.62	1.00	11	69%	0.12	0.06							0.4	−1.0
Van7-96-28	Lherz	Sulf on Cpx cleavage	Sulf6	44	22	0.29%	0.51	0.1357	0.0012	9.5	1%	215	2.04	0.05	528	5%	11.99	0.12	39.096	0.084	15.593	0.026	19.573	0.114	0.2	−0.9
Van7-96-28	Lherz	Sulf on Cpx cleavage	Sulf7	33	44	0.15%	1.32	0.1339	0.0011	7.5	1%	228	0.83	0.02	405	6%	12.27	0.16	39.204	0.084	15.608	0.026	19.640	0.114	0.7	−0.7
Van7-96-38	Lherz	Sulf on Cpx cleavage	Sulf5	44	20	0.32%	0.46	0.1306	0.0011	2.9	2%	65	0.67	0.02	43	37%	0.97	0.12	37.589	0.084	15.500	0.026	18.115	0.114	0.4	−0.2
Van7-96-38	Lherz	Sulf on edge & inside Cpx	Sulf6	46						1.6	4%	34			40	38%	0.87	0.12	37.678	0.084	15.505	0.026	18.003	0.114		

[a] The largest source of error is due to uncertainty in the blank composition. For Os and Re, the uncertainty due to the blank composition is assumed to be 50%. For Pb, blank uncertainty is the standard error of 6–10 blank analyses.

[b] T_{MA} is the separation time from chondritically-evolving mantle; T_{RD} is the minimum age for Re depletion; both are calculated following Shirey and Walker (1998) and using the composition of PUM from Meisel et al. (1996).

and Shanks, 2003; Alard et al., 2005; Klein and Bach, 2009). Sulfides produced by alteration can be distinguished from mantle sulfides by detailed petrographic and compositional analysis (Luguet et al., 2003, 2004; Klein and Bach, 2009). In Fig. 1D, the sulfide is of probable hydrothermal origin, consisting of pentlandite and chalcopyrite with a rim of magnetite and surrounded by serpentinized olivine. These types of sulfides were avoided when selecting grains for isotopic analysis.

Major element data for Gakkel and SWIR sulfides indicate a predominant mineralogy of pentlandite with minor pyrrhotite and chalcopyrite. In an electron microprobe survey of sulfides in thin sections for eight SWIR peridotites, we found that 16 were pentlandites (28–44% Fe, 13–38% Ni, 33–37% S), while one grain from a pyroxenite vein was chalcopyrite. Liu et al. (2009) analyzed sulfides in 11 Gakkel peridotites by electron microprobe. They found that 31 of 42 sulfides consisted of pentlandite with minor pyrrhotite and/or chalcopyrite, while the other 11 grains were pyrrhotite or chalcopyrite. Quantitative microprobe data were not collected on the sulfides used for isotopic analysis in this study, as carbon coating would have contaminated the grains. However, preliminary standard-addition ICPMS analysis of Fe–Cu–Ni–Co solutions collected during column chemistry indicates that the sulfides are pentlandite with minor amounts of chalcopyrite and pyrrhotite.

In this study, a total of 21 sulfides from 13 Gakkel and SWIR peridotites were extracted for Re–Os and Pb isotopic analysis (Table 1). One sulfide per sample was analyzed for the seven Gakkel peridotites, while multiple (2–4) grains were analyzed for five of the six SWIR peridotites. The difference in number of sulfides per sample is due to the limited availability of material from the Gakkel and does not reflect any systematic difference in modal abundance or grain size between the two ridges. All sulfides were extracted from polished slabs and the petrography of each sulfide was studied prior to removal (Table 1).

Examples of petrographic relationships for sulfides in this study are shown in Fig. 1. The morphologies of Gakkel and SWIR sulfides are similar to previous studies of abyssal peridotite sulfides (Alard et al., 2000; Luguet et al., 2003; Harvey et al., 2006; Liu et al., 2009), occurring as both inclusions in silicate minerals and as interstitial phases. Out of 21 sulfides, seven grains were inclusions in clinopyroxene, one was an inclusion in orthopyroxene and the remaining 12 were interstitial grains (Table 1). Based on petrographic observations, only the sulfide included in orthopyroxene (sample PS59-317-6) is likely to be of residual origin, while the remainder of the sulfides are metasomatic in origin. Fig. 1A demonstrates the lack of distinction that often occurs between intergranular and inclusion sulfides, as the intergranular sulfides continue into the clinopyroxene grain as inclusions, with all grains being interpreted as metasomatic in origin.

4. Methods

Re–Os–Pb were extracted from sulfides using the Re–Os method for diamond sulfides (Pearson et al., 1998; Pearson and Shirey, 1999), with modifications to include separation and analysis of Pb. To extract sulfides, hand-polished slabs of peridotite were prepared and studied petrographically to document the relationships between sulfides and adjacent minerals. Grains were removed from slabs using a diamond scribe to etch around and under the grain. Each grain was cleaned by ultrasonicating in double-distilled acetone followed by Milli-Q water. Grains were weighed to 1 μg precision (Table 1) and spiked for ^{185}Re–^{190}Os. Dissolution and simultaneous micro-distillation of Os were done using chromic–sulfuric acid, with collection of Os in HBr. The remaining solution was spiked with ^{205}Pb and passed through anion exchange resin (AG1x8) columns, using 1N HCl as the eluant. During the primary separation, Fe–Cu–Ni–Co, Re, and Pb were separated. The Pb solutions were then passed again through the columns for further purification.

Analysis of Re concentration by isotope dilution was initially done using the modified 15 in. radius thermal ionization mass spectrometer (TIMS) at the Department of Terrestrial Magnetism (DTM), with Re loaded on Pt filaments and ionized as ReO_4^-. Following the acquisition of a Nu Plasma multi-collector inductively coupled mass spectrometer (MC-ICPMS) and decommissioning of the 15 in. radius TIMS, Re analysis was transferred to the Nu Plasma. For the MC-ICPMS analyses, Re was dissolved in HNO_3, injected as a wet plasma, and measured in static mode on the ion counters. Sample amounts varied from 0.1 to 43 pg (Table 1) and blanks varied from 63 to 425 fg, depending on the reagent batch. In general, blanks contribute $<8\%$ to the total Re measured (Table 1). Some of the very small sulfides have higher concentration blanks: the blank is 38% for a sulfide with 1 ppb Re and 16–19% for three sulphides that have 3–82 ppb Re.

Os analyses were initially carried out using the 15 in. radius TIMS and subsequently transferred to the ThermoFisher Triton TIMS when the 15 in. instrument was decommissioned. In both cases, Os was loaded on Pt filaments, metallized, ionized as OsO_3^- and measured in dynamic mode on a single, discrete-dynode, secondary electron multiplier (SEM). Measured OsO_3^- ratios were corrected to a value of 3.0857 for $^{192}OsO_3/^{188}OsO_3$. Total Os blanks varied from 7 to 66 fg and sample amounts from 0.3 to 328 pg. The blank represents $<1\%$ of measured Os, with the exception of the two sulfides with <1 pg Os, for which the blank is 13% and 20% (Table 1).

Repeat measurements ($n=15$, with uncertainties reported as two standard deviations) of the DTM J-M Os Standard, in amounts of 0.2–1 ng on the Triton SEM, gave $^{186}Os/^{188}Os=0.1198\pm0.0016$, $^{187}Os/^{188}Os=0.1741\pm0.0015$, $^{189}Os/^{188}Os=1.2192\pm0.0065$, $^{190}Os/^{188}Os=1.9877\pm0.0019$, and $^{192}Os/^{188}Os=3.0897\pm0.0131$. For comparison, Luguet et al. (2008) reported 14 repeat analyses of DTM J-M Os, in amounts of 10–100 ng measured using the Triton Faraday cups, as $^{186}Os/^{188}Os=0.1200$, $^{187}Os/^{188}Os=0.1739$, $^{189}Os/^{188}Os=1.2197$, and $^{190}Os/^{188}Os=1.9838$.

Pb was analyzed with the Triton TIMS in peak switching mode on the SEM, using Re filaments and G&H silica gel emitter (Gerstenberger and Haase, 1997). Replicate analyses (reported uncertainties are 2σ standard errors of the population of 14 repeats) of the NBS981 standard give $^{206}Pb/^{204}Pb=16.933\pm0.024$, $^{207}Pb/^{204}Pb=15.470\pm0.024$, and $^{208}Pb/^{204}Pb=36.595\pm0.054$. All data were normalized to the accepted value for NBS981 from Todt et al. (1996): $^{206}Pb/^{204}Pb=16.936$, $^{207}Pb/^{204}Pb=15.489$, and $^{208}Pb/^{204}Pb=36.701$. The 2σ standard errors for the isotope ratios reported in Table 1 are based on the standard errors among 6–10 blank analyses per group of samples, which varied from 0.2% to 0.6%; this error is larger than any uncertainty due to count statistics.

Procedural blanks for Pb were 22–25 pg, based on 6–10 blank analyses per group of samples. Apart from the first group, which only consisted of one sample (PS86-6-38), the groups consisted of 4–10 samples. Sulfide Pb amounts ranged from 11 to 1026 pg, corresponding to a 2–70% blank contribution, with data discarded at $>70\%$ blank. The average composition of the blanks ($n=18$) was $^{206}Pb/^{204}Pb=18.480\pm0.075$, $^{207}Pb/^{204}Pb=15.653\pm0.020$, and $^{208}Pb/^{204}Pb=38.245\pm0.061$. While the blank amount is large relative to the size of some samples, the effect of the blank correction (Fig. 2) is to move samples closer to the MORB array known as the northern hemisphere reference line (NHRL; Hart, 1984). The biggest influence of the blank is on $^{207}Pb/^{204}Pb$ (Fig. 2). The large blanks are due to the use of 20 μL $CrO_3-H_2SO_4$ to distill Os, which contributes

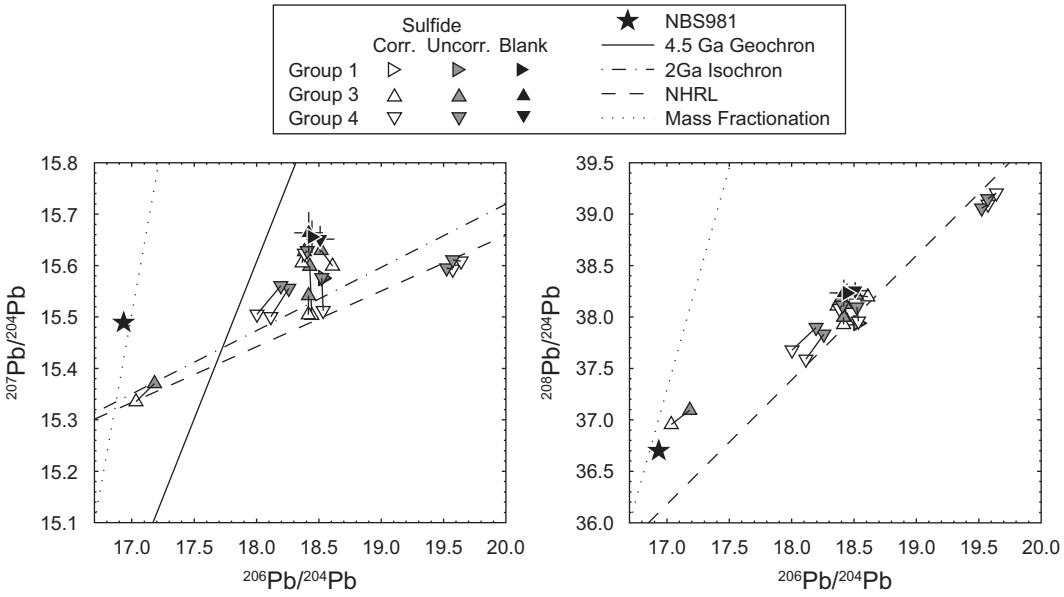

Fig. 2. Blank-corrected and blank-uncorrected Pb isotopic compositions of the sulfides. The uncorrected values (grey symbols) plot closer to the blanks (black symbols) and are connected by tie-lines to their corrected values (white symbols). The corrected values lie closer to the model 2 Ga secondary isochron and the northern hemisphere reference line (NHRL; Hart, 1984), along which most oceanic basalts plot. The star shows the location of NBS981, the Pb isotopic standard used in this study (Todt et al., 1996). The difference between this accepted composition and the average and 2σ standard error of 14 repeat measurements is smaller than the symbol size.

10–17 pg Pb to the procedural blank. No method is currently available to further clean CrO_3 with respect to Pb.

5. Results

Pb, Os, and Re were analyzed in 21 sulfide grains, weighing from 3 to 285 μg, from 13 abyssal peridotites (Table 1). For some sulfides, Pb data are not available due to Pb contamination during the analysis of one group of samples; Os data are not available for a few of the sulfides due to filament failure during metallization.

5.1. Pb, Os, and Re concentrations in sulfides

Measured Pb concentrations in peridotite sulfides vary from 0.12 to 12 ppm (Fig. 3) and average 4 ppm. Some samples with higher Pb concentrations (>1 ppm) from dredge Van7-96 may have interacted with melts related to Bouvet hotspot, based on high clinopyroxene trace element concentrations, enriched Sr–Nd isotopic compositions and proximity to the hotspot track (Warren et al., 2009). Other high Pb samples have no evidence for such melt addition. The large concentration range among samples indicates small scale heterogeneity, including four sulfides from sample Van7-85-49 that range from 0.12 to 5.79 ppm Pb.

Most sulfides have Os concentrations in the range of 0.1–10 ppm and Re concentrations in the range of 0.01–1 ppm (Table 1), within the range for previous abyssal peridotite sulfide studies (Alard et al., 2000; Luguet et al., 2001; Harvey et al., 2006). Pb concentrations are correlated with Os concentrations, with a correlation coefficient of 0.79 among all samples and a correlation coefficient of 0.94 for Gakkel samples (Fig. 3). The SWIR samples are more scattered, probably due to equilibration with Bouvet-derived melts (le Roex et al., 1983; Standish et al., 2008; Warren et al., 2009). Concentrations are not different between the SWIR dredge closer to the Bouvet hotspot track (Van7-96) and the dredge further away (Van7-85). Some of the most elevated Re concentrations are probably due to seawater alteration, as previously reported by Harvey et al. (2006) for sulfides with elevated $^{187}Re/^{188}Os$ but normal $^{187}Os/^{188}Os$.

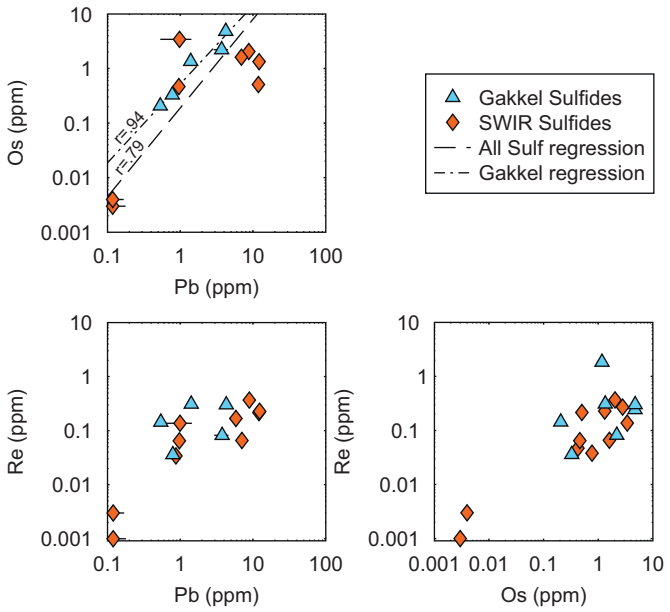

Fig. 3. Co-variation of Pb, Os, and Re concentrations in sulfides from abyssal peridotites. Pb and Os are correlated, with Gakkel samples having a stronger correlation than the combined dataset. The scatter among SWIR sulfides is probably due to recent interaction with melts related to Bouvet hotspot (Standish et al., 2008; Warren et al., 2009). The lack of a correlation between Re and either Pb or Os may reflect recent addition of Re during hydrothermal alteration (Harvey et al., 2006).

5.2. Isotopic composition of the sulfides

The Pb isotopic composition of peridotite sulfides extends over a range larger than global MORB, but similar to the range of orogenic and xenolith peridotites (Fig. 4). One Gakkel sulfide, as well as clinopyroxene from a SWIR sample (Warren et al., 2009), is unradiogenic and plot to the left of the 4.53 Ga reference isochron, which is also referred to as the geochron. The only other published Pb isotopic datasets for abyssal peridotites are the studies by

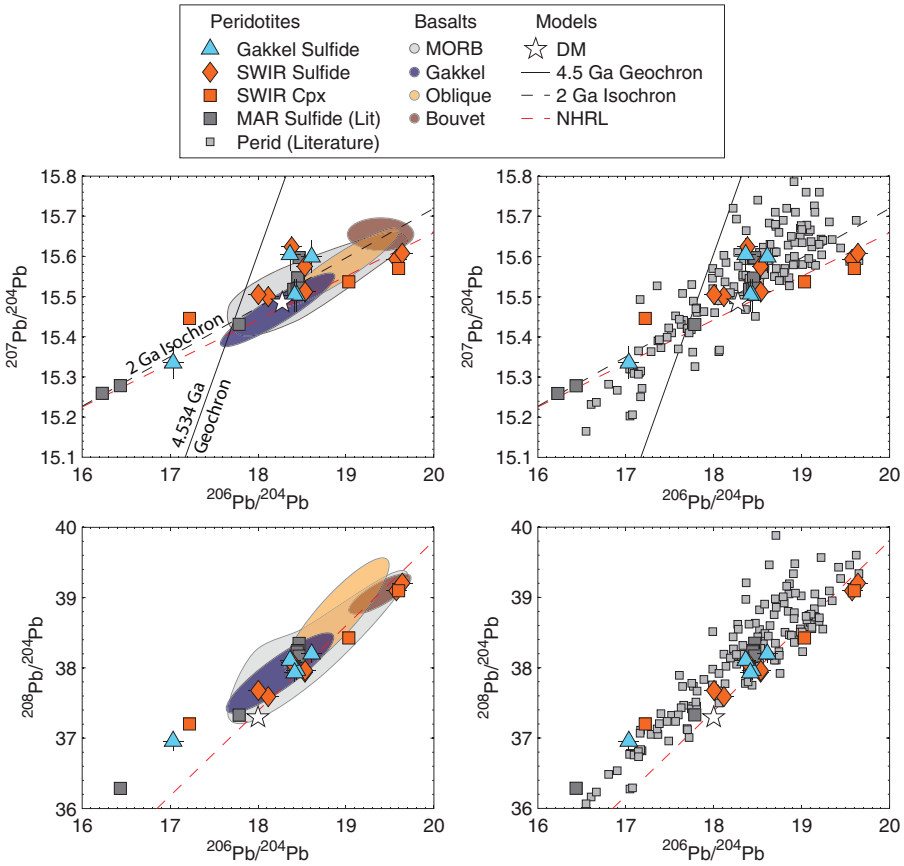

Fig. 4. The variation in Pb isotopic composition of individual sulfide grains extracted from abyssal peridotites. Data for two clinopyroxene mineral separates from SWIR peridotites (Warren et al., 2009) and for MAR sulfides (Burton et al., 2012) are also shown. In the left panels, the grey shaded field outlines the general field for MORB (from PetDB; Lehnert et al., 2000), while the other fields outline basalts from the Gakkel Ridge (Goldstein et al., 2008), SWIR Oblique Segment (Standish, 2006; Standish et al., 2008) and Bouvet Island (Warren et al., 2009). In the right panels, sulfides are compared to literature data for orogenic and xenolith peridotites from whole rock and mineral separate analyses (Hamelin and Allègre, 1988; Meijer et al., 1990; Mukasa et al., 1991; Hauri et al., 1994; Carignan et al., 1996; Rosenbaum et al., 1997; Zangana et al., 1997; Mukasa and Shervais, 1999; Witt-Eickschen et al., 2003; Choi et al., 2005, 2007, 2008; Malaviarachchi et al., 2008). DM is the model composition of the present-day mantle (Zindler and Hart, 1986; Workman and Hart, 2005). The geochron is the reference isochron for mantle evolution, which is calculated assuming that core formation ended at 4.534 Ga (Hart and Gaetani, 2006). The reference 2 Ga secondary isochron is calculated using $\mu = 8.25$ and the NHRL is the northern hemisphere reference line (Hart, 1984).

Roden et al. (1984), Warren et al. (2009), and Burton et al. (2012). Therefore, the background peridotite dataset in Fig. 4 also includes a compilation of whole rock and mineral separate data from orogenic peridotites and xenoliths (see figure caption for references). This dataset was filtered to exclude any metasomatized peridotites.

Peridotite sulfides have little systematic covariation with basalt Pb isotopic compositions from the same area of the ridge (Fig. 4). The Gakkel sulfides extend over the full range of Gakkel basalt compositions, without reflecting the isotopic divide identified in basalts at 15°E (Goldstein et al., 2008). For SWIR Oblique Segment peridotites, the sulfides extend to the composition of Bouvet Island basalts, similar to Oblique Segment basalts. However, they also extend to more depleted compositions than associated basalts. SWIR samples show a rough correlation between sulfide Pb isotopic compositions and clinopyroxene Sr and Nd isotopic compositions (Fig. 5).

Sulfide $^{187}Os/^{188}Os$ ranges from 0.1162 to 0.1500, while $^{187}Re/^{188}Os$ covers a large range from 0.20 to 3.36. In general, sulfides with $^{187}Re/^{188}Os > 1$ are interpreted to be high because of recent Re addition during hydrothermal circulation of seawater (Harvey et al., 2006). Not considering these, most sulfides cluster along a 2 Ga model age isochron (Fig. 6). Some samples plot lower than the fertile, undepleted mantle (the primitive upper mantle composition known as PUM; Meisel et al., 1996). Os isotopic compositions are correlated with Pb isotopic compositions (Fig. 7), as are the concentrations of these two elements (Fig. 3), both of which have not been observed previously.

The fidelity of the technique used in this study to determine Pb isotopic compositions is demonstrated by the agreement of results for sulfides from Van7-96-28 with previous data collected on this sample by two independent analytical techniques. Warren et al. (2009) measured two sulfides from Van7-96-28 by multi-collector ion microprobe and found an average sulfide composition of $^{207}Pb/^{206}Pb = 0.791$ and $^{208}Pb/^{206}Pb = 1.998$ (ion microprobe data are normalized to ^{206}Pb, because the ^{204}Pb signal is very small). In this study, the average ratios for two Van7-96-28 sulfides measured by TIMS are $^{207}Pb/^{206}Pb = 0.796 \pm 0.005$ and $^{208}Pb/^{206}Pb = 1.997 \pm 0.009$. Finally, the clinopyroxene mineral separate measured by TIMS by Warren et al. (2009) has a composition of $^{207}Pb/^{206}Pb = 0.794 \pm 0.001$ and $^{208}Pb/^{206}Pb = 1.995 \pm 0.002$.

5.3. Effect of alteration on sulfide compositions

Results of previous studies suggest that the Pb and Os compositions of sulfides are minimally affected by seawater alteration, while Re abundance is sometimes modified. Luguet et al. (2003) found that at low degrees of alteration, sulfides preserve their high-temperature major element compositions. They also observed that bulk rock platinum group elements (including Os) are not significantly redistributed by hydrothermal

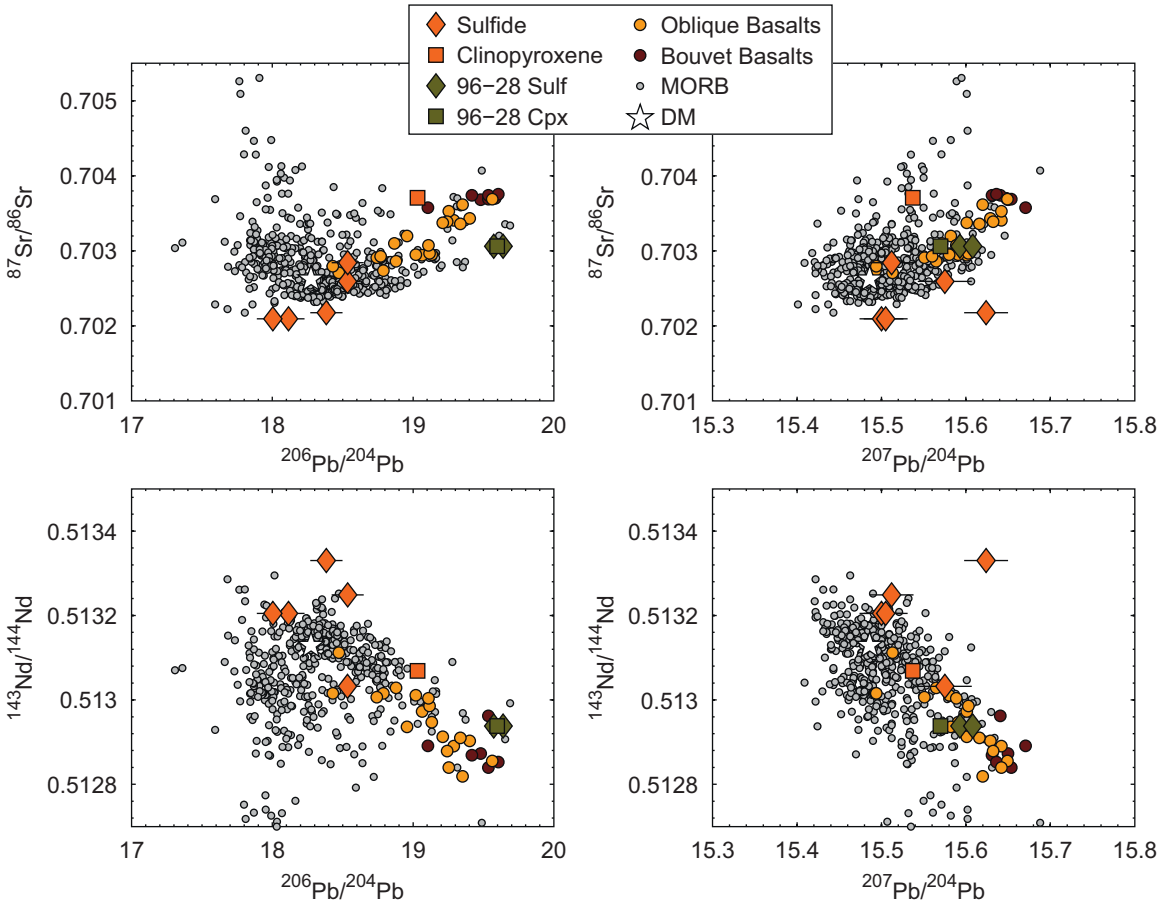

Fig. 5. Comparison of sulfide Pb isotopic compositions to clinopyroxene Sr and Nd isotopic compositions in the same peridotite. All samples are from the SWIR Oblique Segment; clinopyroxene data, along with references for basalt data, are from Warren et al. (2009). Peridotite Van7-96-28 (green symbols) is highlighted to emphasize the fidelity of the sulfide approach for measuring Pb isotopes, as the sulfides reproduce a previous measurement for clinopyroxene (Warren et al., 2009). The enrichment in this sample and others from dredge Van7-96, as well as basalts from the Oblique Segment (Standish et al., 2008), is associated with nearby Bouvet hotspot. (For interpretation of the references to color in this figure caption, the reader is referred to the web version of this article.)

alteration, except for Pd and Au at extreme degrees of alteration. Studies by Snow and Reisberg (1995), Alard et al. (2005), and Harvey et al. (2006) also found that Os is relatively unaffected by alteration, though Re addition can occur. Studies of the Pb isotopic composition of hydrothermal vent deposits have found that these generally have the same composition as that of associated basalts or show minor mixing with seafloor sediments (German et al., 1993; Yao et al., 2009). Serpentinites also have similar compositions to associated basalts, though $^{207}Pb/^{204}Pb$ can be elevated (Deschamps et al., 2012). This suggests that hydrothermal circulation is unlikely to significantly shift the isotopic composition of abyssal peridotite sulfides, though bulk rock Pb concentrations can be increased by the presence of serpentine (Deschamps et al., 2011; Kodolányi et al., 2012).

In this study, a few lines of evidence indicate that sulfide Pb and Os compositions are unaffected by alteration and thus reflect magmatic/mantle compositions. Peridotites have relatively low degrees of hydrothermal alteration, with one Gakkel sample being unaltered (PS59-235-17) and the rest retaining their original mineralogy with $<50\%$ serpentinization. The sulfide from PS59-235-17 plots in the middle of the sulfide range (Fig. 4), similar to sulfides from altered peridotites (HLY102-70-91 and Van7-85-49). Sulfide Pb isotopes overlap global MORB, though with a slight elevation in $^{207}Pb/^{204}Pb$ (Fig. 4). While this could reflect the same hydrothermal alteration effect as observed in serpentine (Deschamps et al., 2012), this more likely reflects the effect of the large Pb blanks, which also have elevated $^{207}Pb/^{204}Pb$ (Fig. 2).

Another line of evidence that seawater alteration has not affected sulfide Pb and Os compositions is the correlation of sulfide Pb and Os concentrations (Fig. 3) and isotopes (Fig. 7). Seawater contamination would produce more scatter, as alteration would not systematically change these elements together. The enriched Os and Pb composition of a subset of sulfides must therefore be indigenous to these sulfides. In this case, it must be due to an enriched mantle component, which is probably the same one that contributes to the elevated Os isotopic composition typical of many MORBs (Alard et al., 2005; Gannoun et al., 2007). In contrast, Re concentrations do not correlate with either Os or Pb (Fig. 3). Re/Os ratios are high among a subset of sulfides, which do not have correspondingly high $^{187}Os/^{188}Os$ (Fig. 6). These two observations suggest that hydrothermal alteration has modified Re but not Os, similar to the observation of Harvey et al. (2006).

Two sulfides were analyzed in an abyssal peridotite (Van7-96-28) for which clinopyroxene Pb isotopic data were collected by Warren et al. (2009). The sulfides have identical Pb isotopic compositions to clinopyroxene and all three points overlap the composition of Bouvet Island basalts (Fig. 4). This overlap agrees with the interpretation that Van7-96-28 and other samples from this dredge were influenced by passage of Bouvet hotspot around 15 Ma (Hartnady and le Roex, 1985; Standish et al., 2008; Warren et al., 2009). The enriched Pb isotopic composition of the sulfides and clinopyroxene also correspond to the elevated Sr and Nd isotopic composition of clinopyroxene from this sample

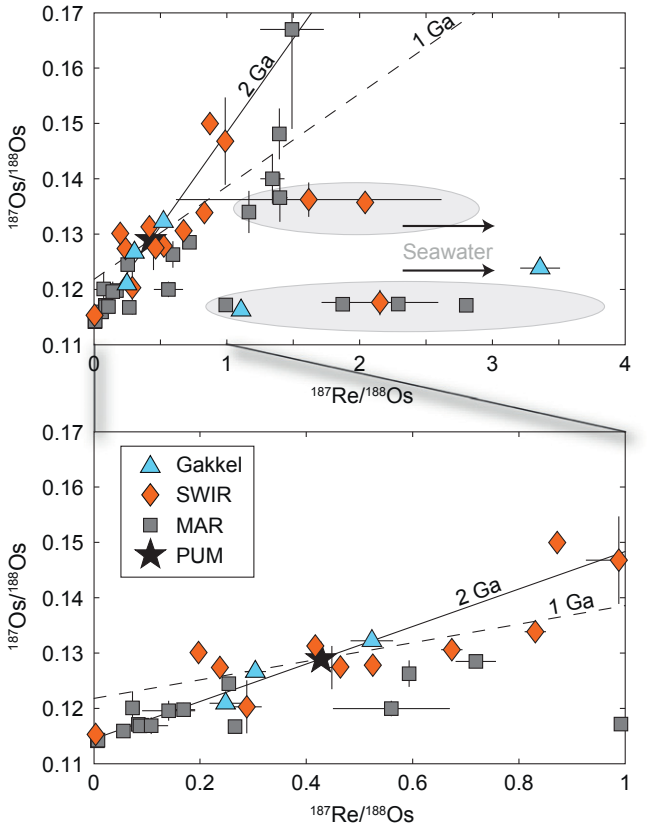

Fig. 6. The Re–Os isotopic composition of sulfides, including MAR and SWIR data from Alard et al. (2005) and Harvey et al. (2006). The isochrons represent Re model ages for primitive upper mantle (PUM) to evolve to its estimated present-day ratios of $^{187}Re/^{188}Os=0.428$ and $^{187}Os/^{188}Os=0.1290$ (Shirey and Walker, 1998). Sulfides align along a 2 Ga model age line, particularly among the more unradiogenic sulfides. The scatter towards higher Re/Os ratios represents seawater alteration, while the scatter towards supra-chondritic $^{187}Os/^{188}Os$–$^{187}Re/^{188}Os$ along the model age lines reflects melt-rock interaction.

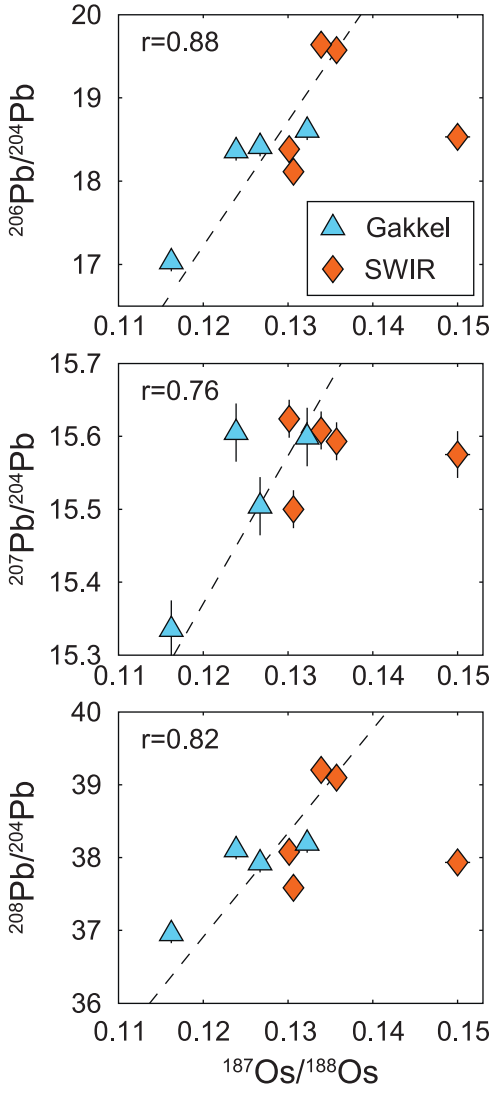

Fig. 7. Co-variation of Pb isotopes with $^{187}Os/^{188}Os$. The dashed lines are regressions through the data and the correlation coefficient is given by *r*. The regressions do not include the high $^{187}Os/^{188}Os$ sulfide from sample PS86-6-38, which is excluded due to radiogenic Os that reflects recent interaction with melts from Bouvet hotspot.

(green symbols in Fig. 5), which overlap Bouvet basalts. The agreement between sulfide and clinopyroxene Pb isotopic compositions and their agreement with basalt data indicate that seawater alteration has not affected the Pb isotopic composition of sulfides.

6. Discussion

6.1. Pb storage in mantle phases

Previous studies have demonstrated that peridotite sulfides contain most of the Os budget of the upper mantle (Hart and Ravizza, 1996; Alard et al., 2000; Harvey et al., 2006, 2011). Based on the Pb concentration in pyroxenes and bulk rocks, mantle Pb has also been suggested to predominantly reside in sulfides (Meijer et al., 1990; Hart and Gaetani, 2006). If sulfides are the main mantle Pb reservoir, then Hart and Gaetani (2006) calculated that they should be ~0.07% abundant and contain ~75 ppm Pb.

Results from this study indicate that sulfides are not the main host for mantle Pb, at least in peridotites with this petrogenetic history. Combining the average sulfide Pb concentration of 4 ppm (Table 1) with an average sulfide mode of 0.02% (Luguet et al., 2001, 2003) gives a bulk peridotite Pb concentration of 0.8 ppb. For comparison, the estimated composition of PUM is 150 ppb (McDonough and Sun, 1995) and of the depleted mantle (DM) is 21 ppb (Salters and Stracke, 2004; Workman and Hart, 2005). Thus, these sulfides would contribute <4% of Pb to typical DM. Using the maximum modal estimate of 0.06% for mantle sulfides determined by Luguet et al. (2003) and our maximum sulfide Pb concentration of 12 ppm, sulfides can still only contribute <8 ppb to the total mantle Pb budget. This corresponds to ~40% of Pb in DM, but this value represents concentrations occurring in samples with melt refertilization.

The range of sulfide Pb concentrations (120 ppb–12 ppm) indicates that mantle sulfides have far lower concentrations than the previous estimate of 75 ppm by Hart and Gaetani (2006). This estimate was based on data for Pb concentrations in peridotite bulk rocks and silicate mineral separates by Meijer et al. (1990). However, the Meijer study compared bulk rock Pb concentrations in different samples to those used to reconstruct bulk rock compositions based on mineral separate data and mineral modes. As bulk rock Pb concentrations vary from 31 to 570 ppb in the Meijer study, combining data from different samples to determine the missing Pb component is probably the cause of the high estimate for sulfide Pb concentrations in the Hart and Gaetani study.

Recently, Burton et al. (2012) also suggested that sulfides are the main host for mantle Pb, based on analyses of sulfide Pb concentrations in an abyssal peridotite. Sulfides in their study have an average concentration of 5 ± 2 ppm ($n=8$), which is slightly higher than the 4 ppm average in this study, but again far lower than the Hart and Gaetani estimate. All their sulfide data come from a single, sulfide-rich section of a drill core from the Fifteen-Twenty Fracture Zone. Burton et al. did not measure Pb concentrations in the bulk abyssal peridotite sample or individual silicate phases. Instead, they measured individual mineral phases in a continental xenolith of garnet harzburgite. This data indicates that sulfides contain $<2\%$ of the bulk rock Pb, whether calculated relative to the measured or the reconstructed bulk peridotite composition. Using a relatively high modal proportion (0.08%) and the maximum measured sulfide Pb concentration, Burton et al. estimated that sulfides store up to 70% of Pb in DM containing 18 ppb Pb, which clearly must be an upper limit estimate. Instead, if their average Pb concentration of 5 ppm is combined with a modal estimate of 0.02% (Luguet et al., 2001, 2003), sulfides correspond to only 5% of Pb in DM.

In contrast, Carignan et al. (1996) measured the bulk rock composition of two peridotite xenoliths, as well as the composition of all silicate phases. Olivine in their study has an average Pb concentration of 11 ppb, orthopyroxene an average of 20 ppb, and clinopyroxene an average of 470 ppb. Combined with mineral modes, the reconstructed whole rock concentrations (21 and 29 ppb) are very similar to the measured whole rock concentration (16 and 40 ppb, respectively). This agreement is particularly striking given the errors associated with such low concentration analyses. Thus, the three main silicate phases in peridotites can account for mantle Pb concentrations with only a minor contribution from sulfide.

In this study, the measured bulk rock Pb concentration for abyssal peridotite Van7-85-49 is 31 ppb, determined by solution-ICPMS at WSU Geoanalytical Laboratory. This concentration corresponds closely to the reconstructed bulk rock Pb concentration of 22 ppb, calculated from mineral modes (72% olivine, 22% orthopyroxene, 5% clinopyroxene, and 1% spinel) and Pb concentration data of 2 ppb for clinopyroxene and 100 ppb for orthopyroxene from Warren et al. (2009). While olivine Pb concentration data are not available, it would only need to be $\sim$13 ppb for the reconstructed and measured concentrations to be in agreement. This value is not unreasonable, but clearly further investigations of abyssal peridotite Pb concentrations are necessary to fully constrain the silicate phase contributions to mantle Pb storage.

Our estimated abyssal peridotite Pb concentration of $\sim$30 ppb is slightly higher than the estimated concentration of 21 ppb Pb in DM (Salters and Stracke, 2004; Workman and Hart, 2005). Abyssal peridotites should contain less Pb than DM, as Pb is incompatible during melting. Retention of Pb in sulfides does not provide an explanation for the higher Pb in abyssal peridotites compared to DM, based on our estimate that sulfides contain <1 ppb Pb. One possible explanation is that abyssal peridotite and DM estimates are only correct within an order of magnitude—i.e., both contain $\sim$10's of ppb Pb. The estimated concentration of Pb in DM may be too low, as this value is determined from the assumption of a "canonical" Ce/Pb or Nd/Pb ratio (Salters and Stracke, 2004; Workman and Hart, 2005). The canonical ratio derives from the suggestion that Pb has a similar bulk partition coefficient to Ce or Nd during mantle melting, based on the lack of large variations between these elements in oceanic basalts (Hofmann et al., 1986; Rehkämper and Hofmann, 1997). However, Sims and DePaolo (1997) calculated a bulk peridotite D_{Pb} of $\sim$0.025, placing Pb midway between Ce and Nd in terms of partitioning, from which they derived an estimate of $\sim$38 ppb Pb in DM.

Overall, the measured bulk rock concentrations for peridotites are similar to bulk rock concentrations reconstructed from silicate phases, confirming that sulfides are not a major reservoir for mantle Pb, as was recently shown by Burton et al. (2012). Instead, most Pb in the mantle resides in silicate minerals. However, while the concentrations determined for sulfides are lower than expected, they are high enough to use sulfides as a tracer of mantle Pb isotopic composition.

6.2. Pb partitioning during melting

Both Pb and Os have higher concentrations in sulfides with respect to co-existing silicates, indicating that they are more compatible in sulfides compared to silicates (Shimazaki and MacLean, 1976; Hart and Ravizza, 1996). However, results of this study indicate that sulfide Pb concentrations are lower than previously predicted, suggesting that the compatibility of Pb in sulfides during melting is also lower than expected. The Pb partition coefficient (D_{Pb}) between sulfide melt and silicate melt has not been directly measured, but was previously estimated to be $\sim$200 (Hart and Gaetani, 2006).

In this study, Pb and Os in sulfides are reasonably well correlated (Fig. 3), with a correlation coefficient of 0.79, based on a York least squares regression of $\log_{10}$[Os] against $\log_{10}$[Pb] (York, 1966). This correlation can be used to estimate D_{Pb} by combining the concentration correlation with D_{Os} and a simple fractional melting model (Minster and Allègre, 1978; Sims and DePaolo, 1997; Workman and Hart, 2005). Os is compatible in sulfide melts compared to silicate melts, with D_{Os} estimated as 5×10^4 from sulfide globules in basaltic glass (Roy-Barman et al., 1998). Experimental studies have found a wider range of Os partition coefficients, from 10^2 to 10^7 as a function of oxygen fugacity, but also suggest that $D_{Os} = 10^4$ for upper mantle conditions (Fleet et al., 1996; Fonseca et al., 2011).

Given uncertainty in D_{Os} and scatter in the sulfide concentration plot (Fig. 3), a modal fractional melting model is appropriate for estimating D_{Pb}

$$\frac{C^s_{Pb}}{C^i_{Pb}} = (1-F)^{((1/D_{Pb})-1)} \tag{1}$$

where C^i_{Pb} is the initial concentration of Pb and C^s_{Pb} is the concentration in the solid after melt fraction F. A similar equation can be written for Os and the two equations equated by solving for F. The result is linearized as follows:

$$\log_{10}(C^s_{Pb}) = M \log_{10}(C^s_{Os}) + \log_{10}\left[\frac{C^i_{Pb}}{(C^i_{Os})^M}\right] \tag{2}$$

where M is

$$M = \frac{D_{Os}(1-D_{Pb})}{D_{Pb}(1-D_{Os})} \tag{3}$$

M is also the slope of the regression of $\log_{10}[Pb]$ against $\log_{10}[Os]$ (as shown in Fig. 3, though these regressions have slopes of $1/M$ as [Pb] is plotted on the x-axis). Thus, D_{Pb} can be solved for:

$$D_{Pb} = \left[\frac{(1-D_{Os})}{D_{Os}}M + 1\right]^{-1} \tag{4}$$

This gives $D_{Pb}=2.6$ for $M=0.62$ and $D_{Os}=5 \times 10^4$. This calculation is not sensitive to the value of D_{Os}, which can vary as a function of oxygen fugacity from 10^2 to 10^7 (Fonseca et al., 2011). Across these five orders of magnitude, D_{Pb} only changes in the second decimal place due to the insensitivity introduced by the term $(1-D_{Os})$.

In contrast, D_{Pb} is sensitive to the regression slope M, with $D_{Pb}=3.3$ if only the Gakkel sulfides are used in the regression, for which $M=0.69$. This value of $D_{Pb}=3.3$ may represent a better estimate than $D_{Pb}=2.6$ based on all sulfides. The SWIR samples

have considerable scatter and result in the regression being pinned by two low concentration samples (Fig. 3). The scatter among the SWIR sulfides may be due to the fact that many sulfides are predominantly Mss (or pentlandite–pyrrhotite) but can have minor chalcopyrite. As Os does not partition as strongly into Cu-rich sulfides (Alard et al., 2000; Luguet et al., 2001), the scatter in Os and Pb concentrations may reflect variable amounts of chalcopyrite in the SWIR sulfides.

Overall, the sulfide Pb and Os correlation provide an order of magnitude estimate for D_{Pb} of ~ 3. This confirms that Pb is more compatible in sulfide melts compared to silicate melts, but also that Pb is less compatible than previously estimated. A lower partition coefficient for Pb in sulfide provides an explanation for the relatively low sulfide Pb concentrations measured in this study compared to the prediction by Hart and Gaetani (2006).

6.3. Evolution of mantle composition

In the oceanic mantle, the long-term effect of plate tectonics is the creation of compositional heterogeneities at length-scales ranging from thousands of kilometers (e.g., Hart, 1984; Meyzen et al., 2007) to sub-kilometer (e.g., Shirey et al., 1987; Dosso et al., 1999; Standish et al., 2008; Warren et al., 2009). Sulfides from the same dredge (this study) and from the same drill core (Alard et al., 2005; Harvey et al., 2006; Burton et al., 2012) preserve distinct isotopic compositions at length-scales $\ll 1$ km. This observation is similar to the large compositional range observed among olivine-hosted melt inclusions in basalts (Saal et al., 1998; Kobayashi et al., 2004; Maclennan, 2008). These melt inclusions have been interpreted as demonstrating that melts of distinct compositions can be preserved during the formation of large-volume magmas. Evidence for variability in the melt source region has previously been documented using Nd and Sr isotopes to trace compositional variability among peridotite pyroxene mineral separates from the same dredge (Cipriani et al., 2004; Warren et al., 2009). Sulfide compositional variability thus agrees with the previous evidence for extremely small ($\ll 1$ km) length-scales of mantle heterogeneity and provides further characterization of the nature of the source mantle for basalts.

The compositional variation of the sulfides also demonstrates the ability of recent melt remobilization to modify mantle composition. The absence of a correlation between sulfide Re and Os (Fig. 6) must have occurred recently, as otherwise Re–Os in some sulfides would not give negative ages (Table 1). Warren et al. (2009) made a similar observation with respect to the lack of isochronous relationships for Sm–Nd and Rb–Sr isotopic data for pyroxene mineral separates from SWIR peridotites. Evidence for recent melt refertilization has also been found in the form of mineralogical and major and trace element variations in abyssal peridotites (Elthon, 1992; Niu, 1997; Seyler and Bonatti, 1997; Seyler et al., 2001, 2007; Hellebrand et al., 2002; Brunelli et al., 2006; Dick et al., 2010; Warren and Shimizu, 2010). In this study, the sulfide from sample PS86-6-38 has a very radiogenic Os composition for its corresponding Pb isotopic composition, though this sample plots near the 2 Ga Re model age line (Fig. 6). This sample has relatively high trace element concentrations and high modal clinopyroxene (13%), along with an enriched Nd–Sr isotopic composition (Warren et al., 2009), all of which suggest melt infiltration during the passage of Bouvet hotspot. The excess radiogenic Os in this sample, relative to the Pb and Os isotopic correlation displayed by other samples, may be due to rhenium-enriched material in the hotspot source. This would be expected if this source mantle contained recycled crustal material.

Excluding the sulfide from sample PS86-6-38, sulfide Pb and Os isotopes are correlated, with an average correlation coefficient of 0.8 (Fig. 7). Both systems yield similar model ages: in Fig. 4, the Pb isotopic composition of mantle sulfides aligns along the 2 Ga data array for oceanic basalts and peridotite mineral separates. In Fig. 6, the Re–Os datasets for SWIR, MAR and Gakkel sulfides all plot along the 2 Ga Re model age line. The observation of a Pb–Os isotopic correlation (Fig. 7), a ~ 2 Ga age, and a very small ($\ll 1$ km) length-scale of peridotite compositional variability can be explained either by (1) a predominant depletion event due to crustal extraction at 2 Ga or (2) an average mixing age for the mantle.

If the actual age of mantle depletion and heterogeneity is ~ 2 Ga, this indicates that upper mantle variability directly reflects melting, depletion, and re-mixing of components at this specific time. The sensitivity of Os to melt removal effects, the coupling of Os with Pb, and the small scale of the heterogeneities seen in the sulfide data would then require a major event around 2 Ga. Detrital zircon age distributions document episodic growth of the continental crust with a major crust-building event at 1.9 Ga (Kemp et al., 2006; Condie and Aster, 2010). This continental growth has been proposed to result from super-plume events (e.g., Condie, 1998) or from more pronounced subduction that drove large-volume mantle depletion and crust formation (e.g., Shirey and Richardson, 2011).

If the sulfides reflect an episode of continental crustal growth, then we would expect any of the individual sulfide grains to record the 2 Ga time of melting, as observed for a large number of grains in Fig. 6. However, Fig. 6 also shows that most of our data are derived from only slightly depleted peridotites, with the sulfides varying from chondritic ($^{187}Re/^{188}Os = 0.42$) to supra-chondritic (> 0.42) compositions. Unless all these sulfides have undergone recent metasomatic addition of Re, a single depletion event that can explain the Os data seems unlikely. Furthermore, episodes of peak crustal formation have also been identified at 2.7, 1.0, 0.6, and 0.3 Ga (Condie and Aster, 2010), but sulfide data from three ocean ridges – Gakkel, SWIR and MAR – do not show any other age peaks. In contrast, continental lithospheric mantle records Re–Os model age peaks that correspond to peaks in zircon age distributions (e.g., Pearson et al., 2007).

The alternative possibility for the sulfide array is that depletion is caused by crust extraction, but specific pulses of continental crust formation cannot be mapped out in samples from the convecting mantle. Instead, the sulfide array is an average mixing age over the history of the Earth, reflecting multiple events of oceanic lithosphere formation and recycling. The mixing of ancient components back into the mantle by subduction has long been suggested as an explanation for the heterogeneity of the oceanic basalt array (e.g., Chase, 1981; Hofmann and White, 1982; Zindler and Hart, 1986; Kellogg et al., 2007), as has delamination of subcontinental lithospheric mantle (e.g., Widom et al., 1999; Gao et al., 2002; O'Reilly et al., 2009). While recycled slab components or pieces of subcontinental lithospheric mantle would be distributed on a scale smaller than the source region for MORBs, mixing down to the scale of individual peridotite samples is unlikely. Based on the small length-scale variability in our sulfide dataset, we suggest that trapped melts also play an important role in the generation of heterogeneous oceanic mantle. Melt extraction at ridges is often incomplete, with a residual trapped melt fraction resulting in peridotite refertilization (e.g., Elthon, 1992; Seyler et al., 2001; Hellebrand et al., 2002). Subduction zones also play a role in mantle refertilization, through the addition of components to the mantle wedge.

In this model, sulfide Pb–Os ages reflect the prior multi-stage history of convection as recorded by the oceanic mantle. Sulfides produced during ridge melting events would range from sub-chondritic to supra-chondritic in $^{187}Re/^{188}Os$, as seen in Fig. 6, depending on the degree of melt removal and addition. In this scenario, variability among sulfides is due to previous processing at ancient ridges, with sulfides retaining different $^{187}Re/^{188}Os$ at the sulfide-grain scale through the typical mantle convection cycle. Mantle heterogeneity is thus produced across a range of length-scales by a combination of mantle mixing and melt refertilization. In addition to the small length-scale heterogeneity, a subset of sulfides

have unradiogenic Pb and Os isotopic compositions that confirm the occurrence of depleted reservoirs in the convecting mantle.

6.4. Ultra-depleted reservoirs in the mantle

Results from this study confirm the occurrence of ancient depleted reservoirs in the oceanic upper mantle, which can be sampled in abyssal peridotites but are difficult to observe in MORBs. Recent studies using the isotope systems Sm–Nd (Cipriani et al., 2004), Rb–Sr (Warren et al., 2009), Lu–Hf (Stracke et al., 2011), and Re–Os (Alard et al., 2005; Harvey et al., 2006; Liu et al., 2008; Burton et al., 2012) have all found that abyssal peridotites extend to more depleted compositions than MORBs. In addition, some ridge sections consist of ultra-depleted peridotite with little or no overlying crust, suggesting the occurrence of pre-existing mantle depletion in these regions. The best examples of this are the Fifteen-Twenty Fracture Zone on the MAR (Kelemen et al., 2007; Seyler et al., 2007) and the eastern SWIR between the Melville Fracture Zone and the Rodrigues Triple Junction (Cannat et al., 2003; Seyler et al., 2003).

This study extends the observation of depleted mantle reservoirs in abyssal peridotites to the Pb isotope system, with significant implications for the storage of Pb in the oceanic upper mantle. Sulfides cover the full array of MORB Pb data (Fig. 4), while also extending to more depleted compositions than basalts. The geochron in Fig. 4 is the present-day isochron that tracks the evolution of ^{206}Pb and ^{207}Pb (both are daughter products of U) in the Earth. Oceanic basalts plot almost entirely to the right of the geochron, yet by mass balance there must be material that plots to the left, if the silicate earth has remained a closed system since core formation (e.g., Hofmann, 2003). This unradiogenic material has long been sought and its absence is termed the "first Pb-paradox" (Allègre, 1969).

For peridotites, the geochron does not appear to represent a compositional boundary (Fig. 4). In addition, peridotites extend to the most unradiogenic compositions of any mantle-derived sample (Malaviarachchi et al., 2008; Burton et al., 2012). Combined with evidence from peridotite Nd, Sr, Hf, and Os isotopes, the upper mantle that is sampled at ridges must contain volumetrically large reservoirs of depleted unradiogenic material. The presence of a large volume of unradiogenic Pb in the mantle has also been suggested based on bulk rock trace element concentrations (Godard et al., 2005; Kelemen et al., 2007; Hanghøj et al., 2010) and in a recent study of sulfide Pb isotopes (Burton et al., 2012). In contrast, most other material, such as continental crust, sediments, and oceanic basalts, rarely plot to the left of the geochron. Unradiogenic Pb compositions have been found in some lower crustal xenoliths (Reid et al., 1989) and granulite terrains (Moorbath et al., 1969), suggesting that this is another reservoir for depleted material, though the average composition of lower crustal xenoliths plots to the right of the geochron (Rudnick and Goldstein, 1990).

The peridotite trend in Fig. 4 suggests that the upper mantle contains sizable reservoirs of highly depleted peridotite, as 24% of peridotites plot to the left of the geochron. While roughly a quarter of peridotites are unradiogenic, less than 3% of MORBs plot to the left of the geochron. A caveat to these statistics is that the global Pb dataset for peridotites is restricted in number (153 samples) and geographic extent, so the relative abundance of unradiogenic to radiogenic peridotites may change as more samples are analyzed. However, the difference between the peridotite and MORB datasets with respect to the unradiogenic end of the spectrum is striking (Fig. 4). For refractory mantle domains to be a significant reservoir of the "missing" unradiogenic Pb referred to in the first Pb-paradox depends on three factors: (i) the degree of isotopic depletion of these reservoirs, (ii) the total amount of Pb in these reservoirs, and (iii) the size of these reservoirs. As 24% of peridotites are unradiogenic (Fig. 4), this may indicate that refractory domains form a quarter of the present-day mantle. Improved constraints on Pb concentrations in these domains are necessary before a full mass balance can be carried out.

The decoupling of basalt and peridotite Pb – and Nd, Sr, Hf – isotopic compositions can be explained by a combination of processes. The development of depleted isotopic signatures in the mantle requires the formation of low abundances of parent elements over the previous 100's–1000's of million years. Hence, refractory domains may originate as recycled oceanic lithospheric mantle that was depleted by melt extraction in either a ridge or arc environment. In particular, the upper section of oceanic lithospheric mantle undergoes the highest degrees of melting and has been suggested as the source of ultra-depleted reservoirs based on peridotite trace element systematics (Godard et al., 2005; Kelemen et al., 2007; Hanghøj et al., 2010). Basalts are weaker tracers of recycled lithosphere, but Salters et al. (2011) were able to identify the presence of depleted mantle domains in oceanic basalt sources based on Nd–Hf isotopic trends among hundreds of basalts. After lithospheric mantle is recycled back into the asthenosphere, it may undergo little or no melting beneath the present-day ridge, resulting in a minimal contribution to the isotopic composition of MORB (Liu et al., 2008; Malaviarachchi et al., 2008). In addition, any melt from these domains will contain smaller quantities of Pb relative to melts from more enriched domains, and thus this unradiogenic component will be diluted when these melts mix to form basalts (Warren et al., 2009).

Evidence for unradiogenic Pb in peridotites should be accompanied by other evidence for peridotite depletion. However, the trace and major element composition of peridotites have often been modified by recent melt refertilization (e.g., Elthon, 1992; Seyler et al., 2001; Hellebrand et al., 2002), with the result that isotopic compositions rarely correlate with other parameters of depletion (Warren et al., 2009). In this study, sulfide Pb isotopes roughly correlate with pyroxene Sr and Nd isotopes from the same sample (Fig. 5), but Warren et al. (2009) found no correlation between these Sr and Nd isotopes and other non-isotopic indicators of depletion. In a study of clinopyroxene Hf and Nd isotopes in Gakkel and SWIR peridotites, Stracke et al. (2011) found a correlation between Hf isotope depletion and major and trace element depletion, which their modeling showed reflected a combination of melt depletion and refertilization. Similarly, the highly unradiogenic samples from the Horoman Peridotite are mainly plagioclase lherzolites that have undergone melt refertilization (Malaviarachchi et al., 2008, 2010) and show no correlation between isotopic composition and bulk rock major or trace elements. However, if refertilization was recent and by a melt containing similarly unradiogenic Pb (i.e., a melt from the surrounding area), then this can explain these samples having elevated major and trace element compositions while still recording unradiogenic Pb.

7. Conclusions

The Pb and Re–Os composition of single sulfides from abyssal peridotites have been analyzed to constrain oceanic mantle composition and evolution. Sulfides from the Gakkel ridge and SWIR contain 0.12–12 ppm Pb, 0.001–0.4 ppm Re, and 0.003–5 ppm Os. Hydrothermal alteration has had a minimal effect on sulfide Pb and Os compositions, based on (i) the comparison of sulfides from fresh and partially altered peridotites, (ii) measurement of an identical Pb isotopic composition in sulfide and clinopyroxene from the same sample, and (iii) correlations between Pb and Os isotopes and concentrations. In contrast, Re is not correlated with Pb and Os, with some samples containing high ^{187}Re/^{188}Os at relatively low ^{187}Os/^{188}Os, both of which suggest modification by hydrothermal alteration.

The Pb and Os concentrations of sulfides are correlated and this correlation provides an estimate of ~ 3 for the Pb partition coefficient between sulfide melt and silicate melt. This estimate is lower than previous estimates for sulfide Pb partitioning, indicating that Pb is not as compatible in sulfides as previously suggested. Previous studies have also suggested that sulfides are the main host for mantle Pb. However, a revised comparison of bulk rock and mineral Pb concentrations demonstrates that the majority of peridotite Pb is stored in silicate phases. Results of this study show that sulfides contain < 1 ppb of the total Pb in peridotites, which corresponds to $< 4\%$ of the Pb in DM.

Abyssal peridotite sulfides cover an isotopic range extending from $^{206}Pb/^{204}Pb = 17.0$ to 19.6, $^{187}Os/^{188}Os = 0.116$ to 0.150, and $^{187}Re/^{188}Os = 0.20$ to 3.36. Pb and Os isotopic compositions are correlated, with sulfides in both isotope systems plotting along ~ 2 Ga isochrons. The coupling of Pb and Os, the $\ll 1$ km length-scale of the isotopic variations, and the occurrence of supra-chondritic $^{187}Re/^{188}Os$ support an origin for this "age" by ancient ridge melting and refertilization combined with recycling of oceanic lithosphere back into the mantle, to give an average of ~ 2 Ga.

The Pb isotopic composition of sulfides extends to very depleted compositions that plot to the left of the geochron in a diagram of $^{207}Pb/^{204}Pb$ versus $^{206}Pb/^{204}Pb$. Combined with Pb isotopic data for orogenic and xenolith peridotites, 24% of peridotites are unradiogenic and plot to the left of the geochron, in comparison to only 3% of MORBs. This suggests that the mantle is a major reservoir for unradiogenic Pb, and that, historically, examination of the isotopic composition of only basalts has produced a dataset biased to more radiogenic values. This provides a solution to the first Pb-paradox, depending on the size, concentration and isotopic range of these depleted mantle domains. These domains are suggested to originate from recycling of oceanic lithospheric mantle, which undergoes little or no melting at modern ridges due to its refractory composition. Combined with the low trace element concentration of melts formed from such refractory reservoirs, this component is rarely observed in basalts.

Acknowledgments

R. Carlson, M. Horan, T. Mock, M. Schmitz, N. Shimizu, E. Hauri, A. Saal, and K. Smit are thanked for their useful discussions and advice. P. Kelemen kindly shared his calculations and insight on Pb storage in the mantle. H. Dick provided the Gakkel samples. O. Alard gave constructive comments on a previous version of this paper. A. Luguet, J. Harvey, and T. Elliott are thanked for insightful reviews; T. Elliott is also thanked for thoughtful editorial handling. This work was supported by Stanford University and by Carnegie Institution of Washington, including a Carnegie Postdoctoral Fellowship to J.M.W.; S. Solomon is thanked for additional postdoctoral funding.

References

Alard, O., Griffin, W.L., Lorand, J.-P., Jackson, S.E., O'Reilly, S.Y., 2000. Non-chondritic distribution of the highly siderophile elements in mantle sulphides. Nature 407, 891–894.

Alard, O., Luguet, A., Pearson, N.J., Griffin, W.L., Lorand, J.-P., Gannoun, A., Burton, K.W., O'Reilly, S.Y., 2005. *In situ* Os isotopes in abyssal peridotites bridge the isotopic gap between MORBs and their source mantle. Nature 436, 1005–1008.

Albarède, F., 2001. Radiogenic ingrowth in systems with multiple reservoirs: applications to the differentiation of the mantle-crust system. Earth Planet. Sci. Lett. 189, 59–73.

Allègre, C.J., 1969. Comportement des systèmes U–Th–Pb dans le manteau supérieur et modèle d'évolution de ce dernier au cours des temps géologiques. Earth Planet. Sci. Lett. 5, 261–269.

Allègre, C.J., 1982. Chemical geodynamics. Tectonophysics 81, 109–132.

Allègre, C.J., Brévart, O., Dupré, B., Minster, J.F., 1980. Isotopic and chemical effects produced in a continuously differentiating convecting earth mantle. Philos. Trans. Roy. Soc. Lon. A 297, 447–477.

Alt, J.C., Shanks, W.C., 2003. Serpentinization of abyssal peridotites from the mark area, mid-atlantic Ridge: sulfur geochemistry and reaction modeling. Geochim. Cosmochim. Acta. 67 (4), 641–653.

Bach, W., Garrido, C.J., Paulick, H., Harvey, J., Rosner, M., 2004. Seawater-peridotite interactions: first insights from ODP Leg 209, MAR 15°N. Geochem. Geophys. Geosyst. 5 (9).

Bown, J.W., White, R.S., 1994. Variation with spreading rate of oceanic crustal thickness and geochemistry. Earth Planet. Sci. Lett. 121, 435–449.

Brunelli, D., Seyler, M., Cipriani, A., Ottolini, L., Bonatti, E., 2006. Discontinuous melt extraction and weak refertilization of mantle peridotites at the Vema Lithospheric Section (Mid-Atlantic Ridge). J. Petrol. 47 (4), 745–771.

Burton, K.W., Cenki-Tok, B., Mokadem, F., Harvey, J., Gannoun, A., Alard, O., Parkinson, I.J., 2012. Unradiogenic lead in Earth's upper mantle. Nat. Geosci. 5 (8), 570–573.

Cannat, M., 1993. Emplacement of mantle rocks in the seafloor at mid-ocean Ridges. J. Geophys. Res. 98 (B3), 4163–4172.

Cannat, M., Rommevaux-Jestin, C., Fujimoto, H., 2003. Melt supply variations to a magma-poor ultra-slow spreading ridge (Southwest Indian Ridge from 61° to 69°E. Geochem. Geophys. Geosyst. 4 (8).

Cannat, M., Sauter, D., Mendel, V., Ruellan, E., Okino, K., Escartín, J., Combier, V., Baala, M., 2006. Modes of seafloor generation at a melt-poor ultraslow-spreading ridge. Geology 34, 605–608.

Carignan, J., Ludden, J.N., Francis, D., 1996. On the recent enrichment of subcontinental lithosphere: a detailed U–Pb study of spinel lherzolite xenoliths, Yukon, Canada. Geochim. Cosmochim. Acta. 60 (21), 4241–4252.

Chase, C.G., 1981. Oceanic island Pb: two-stage histories and mantle evolution. Earth. Planet. Sci. Lett. 52, 277–284.

Choi, S.H., Kwon, T.-T., Mukasa, S.B., Sagong, H., 2005. Sr–Nd–Pb isotope and trace element systematics of mantle xenoliths from Late Cenozoic alkaline lavas, South Korea. Chem. Geol. 221, 40–64.

Choi, S.H., Mukasa, S.B., Andronikov, A.V., Marcano, M.C., 2007. Extreme Sr–Nd–Pb–Hf isotopic compositions exhibited by the Tinaquillo peridotite massif, northern Venezuela: implications for geodynamic setting. Contrib. Mineral. Petrol. 153, 443–463.

Choi, S.H., Mukasa, S.B., Zhou, X.-H., Xian, X.H., Andronikov, A.V., 2008. Mantle dynamics beneath East Asia constrained by Sr, Nd, Pb and Hf isotopic systematics of ultramafic xenoliths and their host basalts from Hannuoba, North China. Chem. Geol. 248, 40–61.

Cipriani, A., Brueckner, H.K., Bonatti, E., Brunelli, D., 2004. Oceanic crust generated by elusive parents: Sr and Nd isotopes in basalt-peridotite pairs from the Mid-Atlantic Ridge and Nd isotopes in basalt-peridotite pairs from the Mid-Atlantic Ridge. Geology 32 (8), 657–660.

Condie, K.C., 1998. Episodic continental growth and supercontinents: a mantle avalanche connection?. Earth. Planet. Sci. Lett. 163, 97–108.

Condie, K.C., Aster, R.C., 2010. Episodic zircon age spectra of orogenic granitoids: the supercontinent connection and continental growth. Precambrian Res. 180, 227–236.

Czamanske, G.K., Moore, J.G., 1977. Composition and phase chemistry of sulfide globules in basalt form the Mid-Atlantic Ridge rift valley at 37°N lat. Geol. Soc. Am. Bull. 88, 587–599.

Deschamps, F., Godard, M., Guillot, S., Chauvel, C., Andreani, M., Hattori, K., Wunder, B., France, L., 2012. Behavior of fluid-mobile elements in serpentines from abyssal to subduction environments: examples from Cuba and Dominican Republic. Chem. Geol. 312–313, 93–117.

Deschamps, F., Guillot, S., Godard, M., Andreani, M., Hattori, K., 2011. Serpentinites act as sponges for fluid-mobile elements in abyssal and subduction zone environments. Terra Nova 23, 171–178.

Dick, H.J.B., Lin, J., Schouten, H., 2003. An ultraslow-spreading class of ocean ridge. Nature 426, 405–412.

Dick, H.J.B., Lissenberg, C.J., Warren, J.M., 2010. Mantle melting melt transport and delivery beneath a slow-spreading ridge: the paleo-MAR from 23°15′N to 23°45′N. J. Petrol. 51 (1–2), 425–467.

Dosso, L., Bougault, H., Langmuir, C., Bollinger, C., Bonnier, O., Etoubleau, J., 1999. The age and distribution of mantle heterogeneity along the Mid-Atlantic Ridge (31–41°N). Earth. Planet. Sci. Lett. 170, 269–286.

Dromgoole, E.L., Pasteris, J.D., 1987. Interpretation of the sulfide assemblages in a suite of xenoliths from Kilbourne Hole, New Mexico. Geol. Soc. Am. Spec. Pap. 215, 25–46.

Elthon, D., 1992. Chemical trends in abyssal peridotites: refertilization of depleted suboceanic mantle. J. Geophys. Res. 97 (B6), 9015–9025.

Fleet, M.E., Crocket, J.H., Stone, W.E., 1996. Partitioning of platinum-group elements (Os, Ir, Ru, Pt, Pd) and gold between sulfide liquid and basalt melt. Geochim. Cosmochim. Acta 60, 2397–2412.

Fonseca, R.O.C., Laurenz, V., Mallmann, G., Luguet, A., Hoehne, N., Jochum, K.P., 2012. New constraints on the genesis and long-term stability of Os-rich alloys in the Earth's mantle. Geochim. Cosmochim. Acta 87, 227–242.

Fonseca, R.O.C., Mallmann, G., O'Neill, H.S.C., Campbell, I.H., Laurenz, V., 2011. Solubility of Os and Ir in sulfide melt: implications for Re/Os fractionation during mantle melting. Earth. Planet. Sci. Lett. 311, 339–350.

Gannoun, A., Burton, K.W., Parkinson, I.J., Alard, O., Schiano, P., Thomas, L.E., 2007. The scale and origin of the osmium isotope variations in mid-ocean ridge basalts. Earth. Planet. Sci. Lett. 259, 541–556.

Gao, S., Rudnick, R.L., Carlson, R.W., McDonough, W.F., Liu, Y.-S., 2002. Re–Os evidence for replacement of ancient mantle lithosphere beneath the north china craton. Earth. Planet. Sci. Lett. 198, 307–322.

Gast, P.W., Tilton, G.R., Hedge, C., 1964. Isotopic composition of lead and strontium from Ascension and Gough Islands. Science 145, 1181–1185.
German, C.R., Higgs, N.C., Thomson, J., Mills, R., Elderfield, H., Blusztajn, J., Fleer, A.P., Bacon, M.P., 1993. A geochemical study of metalliferous sediment from TAG hydrothermal mound, 26°08′N Mid-Atlantic Ridge. J. Geophys. Res. 98, 9683–9692.
Gerstenberger, H., Haase, G., 1997. A highly effective emitter substance for mass spectrometric Pb isotope ratio determinations. Chem. Geol. 136, 309–312.
Godard, M., Kelemen, P.B., Hart, S.R., Jackson, M.G., Hanghøj, K., 2005. High Pb/Ce reservoir in depleted, altered mantle peridotites. Eos Trans. Am. Geophys. Union 86 (52), pp. V23D–07.
Goldstein, S.L., Soffer, G., Langmuir, C.H., Lehnert, K.A., Graham, D.W., Michael, P.J., 2008. Origin of a 'Southern Hemisphere' geochemical signature in the Arctic upper mantle. Nature 453, 89–93.
Hamelin, B., Allègre, C.J., 1988. Lead isotope study of orogenic lherzolite massifs. Earth. Planet. Sci. Lett. 91, 117–131.
Hanghøj, K., Kelemen, P.B., Hassler, D., Godard, M., 2010. Composition and genesis of depleted mantle peridotites from the Wadi Tayin Massif, Oman Ophiolite. major and trace element geochemistry, and Os isotope and PGE systematics. J. Petrol. 51, 201–227.
Hart, S.R., 1984. A large-scale isotope anomaly in the Southern Hemisphere mantle. Nature 309, 753–757.
Hart, S.R., Gaetani, G.A., 2006. Mantle pb paradoxes: the sulfide solution. Contrib. Mineral. Petrol. 152, 295–308.
Hart, S.R., Ravizza, G.E., 1996. Os partitioning between phases in lherzolite and basalt. In: Basu, A., Hart, S. (Eds.), Earth Processes: Reading the Isotopic Code. Geophysical Monograph, vol. 95. American Geophysical Union, pp. 123–134.
Hartnady, C.J.H., le Roex, A.P., 1985. Southern Ocean hotspot tracks and the Cenozoic absolute motion of the African, Antarctic, and South American plates. Earth. Planet. Sci. Lett. 75, 245–257.
Harvey, J., Dale, C.W., Gannoun, A., Burton, K.W., 2011. Osmium mass balance in peridotite and the effects of mantle-derived sulphides on basalt petrogenesis. Geochim. Cosmochim. Acta 75, 5574–5596.
Harvey, J., Gannoun, A., Burton, K.W., Rogers, N.W., Alard, O., Parkinson, I.J., 2006. Ancient melt extraction from the oceanic upper mantle revealed by Re–Os isotopes in abyssal peridotites form the Mid-Atlantic ridge. Earth. Planet. Sci. Lett. 244, 606–621.
Hauri, E.H., Wagner, T.P., Grove, T.L., 1994. Experimental and natural partitioning of Th, U, Pb and other trace elements between garnet, clinopyroxene and basaltic melts. Chem. Geol. 117, 149–166.
Hellebrand, E., Snow, J.E., Hoppe, P., Hofmann, A.W., 2002. Garnet-field melting and late-stage refertilization in 'residual' abyssal peridotites from the Central Indian Ridge. J. Petrol. 43 (12), 2305–2338.
Hofmann, A.W., 1997. Mantle geochemistry: the message from oceanic volcanism. Nature 385, 219–229.
Hofmann, A.W., 2003. Sampling mantle heterogeneity through oceanic basalts: Isotopes and trace elements. In: Carlson, R.W. (Ed.), Treatise on Geochemistry, vol. 2. Elsevier, pp. 61–101.
Hofmann, A.W., Jochum, K.P., Seufert, M., White, W.M., 1986. Nb and Pb in oceanic bassalts: new constraints on mantle evolution. Earth. Planet. Sci. Lett. 79, 33–45.
Hofmann, A.W., White, W.M., 1982. Mantle plumes from ancient oceanic crust. Earth. Planet. Sci. Lett. 57, 421–436.
Jacobsen, S.B., Wasserburg, G.J., 1979. The mean age of mantle and crustal reservoirs. J. Geophys. Res. 84, 7411–7427.
Johnson, K.T.M., Dick, H.J.B., Shimizu, N., 1990. Melting in the oceanic upper mantle: an ion microprobe study of diopsides in abyssal peridotites. J. Geophys. Res. 95, 2661–2678.
Kelemen, P.B., Kikawa, E., Miller, D.J., Party, S.S., 2007. Leg 209 summary: processes in a 20-km-thick conductive boundary layer beneath the Mid-Atlantic Ridge 14°–16°N. In: Kelemen, P.B., Kikawa, E., Miller, D.J. (Eds.), Proceedings of the Ocean Drilling PRogram, Scientific Results, vol. 209. Ocean Drilling Program, College Station, TX, pp. 1–33.
Kellerud, G., Yund, R.A., Moh, G.H., 1969. Phase relation in the Cu–Fe–Ni, Cu–Ni–S and Fe–Ni–S systems. Econ. Geol. Monogr. 4, 323–343.
Kellogg, J.B., Jacobsen, S.B., O'Connell, R.J., 2007. Modeling lead isotopic heterogeneity in mid-ocean ridge basalts. Earth. Planet. Sci. Lett. 262, 328–342.
Kemp, A.I.S., Hawkesworth, C.J., Paterson, B.A., Kinny, P.D., 2006. Episodic growth of the Gondwana supercontinent from hafnium and oxygen isotopes in zircon. Nature 439, 580–583.
Klein, E.M., Langmuir, C.H., 1987. Global correlations of ocean ridge basalt chemistry with axial depth and crustal thickness. J. Geophys. Res. 92 (B8), 8089–8115.
Klein, F., Bach, W., 2009. Fe–Ni–Co–O–S phase relations in peridotite-seawater interactions. J. Petrol. 50, 37–59.
Kobayashi, K., Tanaka, R., Moriguti, T., Shimizu, K., Nakamura, E., 2004. Lithium, boron and lead isotope systematics of glass inclusions in olivines from Hawaiian lavas: evidence for recycled components in the Hawaiian plume. Chem. Geol. 212, 143–161.
Kodolányi, J., Pettke, T., Spandler, C., Kamber, B.S., Gméling, K., 2012. Geochemistry of ocean floor and fore-arc serpentinites: constraints on the ultramafic input to subduction zones. J. Petrol. 53, 235–270.
le Roex, A.P., Dick, H.J.B., Erlank, A.J., Reid, A.M., Frey, F.A., Hart, S.R., 1983. Geochemistry, mineralogy and petrogenesis of lavas erupted along the Southwest Indian Ridge between the Bouvet Triple Junction and 11 degrees East. J. Petrol. 24 (3), 267–318.
Lehnert, K., Su, Y., Langmuir, C., Sarbas, B., Nohl, U., 2000. A global geochemical database structure for rocks. Geochem. Geophys. Geosyst. 1, http://dx.doi.org/10.1029/1999GC00026.
Liu, C.-Z., Snow, J.E., Brügmann, G.E., Hellebrand, E., Hofmann, A.W., 2009. Non-chondritic HSE budget in Earth's upper mantle evidenced by abyssal peridotites from Gakkel ridge (Arctic Ocean). Earth. Planet. Sci. Lett. 283, 122–132.
Liu, C.-Z., Snow, J.E., Hellebrand, E., Brügmann, G.E., von der Handt, A.B., Hofmann, A.W., 2008. Ancient, highly heterogeneous mantle beneath Gakkel ridge, Arctic Ocean. Nature 452, 311–316.
Lorand, J.-P., 1985. The behaviour of the upper mantle sulfide component during the incipient alteration of "Alpine"-type peridotites as illustrated by the Beni Bousera (northern Morocco) and Ronda (southern Spain) ultramafic bodies. Tschermaks Mineral. Petrogr. Mitt. 34, 183–209.
Lorand, J.P., 1989a. Abundance and distribution of Cu–Fe–Ni sulfides, sulfur, copper and platinum-group elements in orogenic-type spinel lherzolite massifs of Ariège (northeastern Pyrenees, France). Earth. Planet. Sci. Lett. 93, 50–64.
Lorand, J.P., 1989b. Mineralogy and chemistry of Cu–Fe–Ni sulfides in orogenic-type spinel peridotite bodies form Ariege (Northeastern Pyrenees, France). Contrib. Mineral. Petrol. 103, 335–345.
Lorand, J.-P., Pattou, L., Gros, M., 1999. Fractionation of platinum-group elements and gold in the upper mantle: a detailed study in Pyrenean orogenic lherzolites. J. Petrol. 40, 957–981.
Luguet, A., Alard, O., Lorand, J.P., Pearson, N.J., Ryan, C., O'Reilly, S.Y., 2001. Laser-ablation microprobe (lam)-icpms unravels the highly siderophile element geochemistry of the oceanic mantle. Earth. Planet. Sci. Lett. 189, 285–294.
Luguet, A., Lorand, J.-P., Alard, O., Cottin, J.-Y., 2004. A multi-technique study of platinium group element systematic in some ligurian ophiloitic peridotites, italy. Chem. Geol. 208, 175–194.
Luguet, A., Lorand, J.-P., Seyler, M., 2003. Sulfide petrology and highly siderophile element geochemistry of abyssal peridotites: a coupled study of samples from the Kane Fracture Zone (45°W 23°20N, MARK Area, Atlantic Ocean). Geochim. Cosmochim. Acta 67 (8), 1553–1570.
Luguet, A., Nowell, G.M., Pearson, D.G., 2008. $^{184}Os/^{188}Os$ and $^{186}Os/^{188}Os$ measurements by negative thermal ionisation mass spectrometry (N-TIMS): effects of interfering element and mass fractionation corrections on data accuracy and precision. Chem. Geol. 248, 342–362.
Maclennan, J., 2008. Lead isotope variability in olivine-hosted melt inclusions from Iceland. Geochim. Cosmochim. Acta 72, 4159–4176.
Malaviarachchi, S.P.K., Makishima, A., Nakamura, E., 2010. Melt-peridotite reactions and fluid metasomatism in the upper mantle, revealed from the geochemistry of peridotite and gabbro from the Horoman Peridotite Massif, Japan. J. Petrol. 51, 1417–1445.
Malaviarachchi, S.P.K., Makishima, A., Tanimoto, M., Kuritani, T., Nakamura, E., 2008. Highly unradiogenic lead isotope ratios from the Horoman peridotite in Japan. Nat. Geosci. 1, 859–863.
McDonough, W.F., Sun, S.-s., 1995. The composition of the Earth. Chem. Geol. 120, 223–253.
Meijer, A., Kwon, T.-T., Tilton, G.R., 1990. U-Th-Pb partitioning behavior during partial melting in the upper mantle: implications for the origin of high Mu components and the Pb Paradox. J. Geophys. Res. 95 (B1), 433–448.
Meisel, T., Walker, R.J., Morgan, J.W., 1996. The osmium isotopic composition of the Earth's primitive upper mantle. Nature 383, 517–520.
Meyzen, C.M., Blichert-Toft, J., Ludden, J.N., Humler, E., Mével, C., AlbarèdeAlbarède, 2007. Isotopic portrayal of the Earth's upper mantle flow field. Nature 447, 1069–1074.
Michael, P.J., Langmuir, C.H., Dick, H.J.B., Snow, J.E., Goldstein, S.L., Graham, D.W., Lehnert, K.A., Kurras, G., Jokat, W., Mühe, R., Edmonds, H.N., 2003. Magmatic and amagmatic seafloor generation at the ultraslow-spreading Gakkel ridge, Arctic Ocean. Nature 423, 956–961.
Minster, J.F., Allègre, C.J., 1978. Systematic use of trace elements in igneous processes part III: inverse problems of batch partial melting in volcanic suites. Contrib. Mineral. Petrol. 68, 37–52.
Montési, L.G.J., Behn, M.D., 2007. Mantle flow and melting underneath oblique and ultraslow mid-ocean ridges. Geophys. Res. Lett. 34, L24307.
Montési, L.G.J., Behn, M.D., Hebert, L.B., Lin, J., Barry, J.L., 2011. Controls on melt migration and extraction at the ultraslow Southwest Indian Ridge 10°–16°E. J. Geophys. Res. 116, B10102.
Moorbath, S., Welke, H., Gale, N.H., 1969. The significance of lead isotope studies in ancient, high-grade metamorphic basement complexes, as exemplified by the Lewisian rocks of northwest Scotland. Earth. Planet. Sci. Lett. 6, 245–256.
Mukasa, S.B., Shervais, J.W., 1999. Growth of subcontinental lithosphere: evidence from repeated dike injections in the Balmuccia lherzolite massif, Italian Alps. Lithos 48, 287–316.
Mukasa, S.B., Shervais, J.W., Wilshire, H.G., Nielson, J.E., 1991. Intrinsic Nd, Pb and Sr isotopic heterogeneities exhibited by the Lherz Alpine Peridotite Massif, French Pyrenees. J. Petrol. Spec. Lherzolites Issue, 117–134.
Niu, Y., 1997. Mantle melting and melt extraction processes beneath ocean ridges: evidence from abyssal peridotites. J. Petrol. 38, 1047–1074.
O'Nions, R.K., Hamilton, P.J., Evensen, N.M., 1977. Variations in $^{143}Nd/^{144}Nd$ and $^{87}Sr/^{86}Sr$ ratios in oceanic basalts. Earth. Planet. Sci. Lett. 34, 13–22.
O'Reilly, S.Y., Zhang, M., Griffin, W.L., Begg, G., Hronsky, J., 2009. Ultradeep continental roots and their oceanic remnants: a solution to the geochemical "mantle reservoir" problem. Lithos 211S, 1043–1054.
Oversby, V.M., Gast, P.W., 1970. Isotopic composition of lead from oceanic islands. J. Geophys. Res. 75, 2097–2114.
Pearson, D.G., Parman, S.W., Nowell, G.M., 2007. A link between large mantle melting events and continent growth seen in osmium isotopes. Nature 449, 202–205.

Pearson, D.G., Shirey, S.B., 1999. Isotopic dating of diamonds. In: Lambert, D., Ruiz, J. (Eds.), Application of Radiogenic Isotopes to ore Deposit Research and Exploration. Society of Economic Geologists, pp. 143–171.
Pearson, D.G., Shirey, S.B., Harris, J.W., Carlson, R.W., 1998. Sulphide inclusions in diamonds from the Koffiefontein kimberlite, S Africa: constraints on diamond ages and mantle Re–Os systematics. Earth. Planet. Sci. Lett. 160, 311–326.
Ramdohr, P., 1967. A widespread mineral association, connected with serpentinization. Neues Jahrbuch Fur Mineralogie—Abhandlungen 107, 241–265.
Rehkämper, M., Hofmann, A.W., 1997. Recycled ocean crust and sediment in Indian Ocean MORB. Earth. Planet. Sci. Lett. 147, 93–106.
Reid, M.R., Hart, S.R., Padovani, E.R., Wandless, G.A., 1989. Contribution of metapelitic sediments to the composition, heat production, and seismic velocity of the lower crust of southern New Mexico, USA. Earth. Planet. Sci. Lett. 95, 367–381.
Roden, M.K., Hart, S.R., Frey, F.A., Melson, W.G., 1984. Sr, Nd and Pb isotopic and REE goechemistry of St. Paul's Rocks: the metamorphic and metasomatic development of an alkali basalt mantle source. Contrib. Mineral. Petrol. 85, 376–390.
Rosenbaum, J.M., Wilson, M., Downes, H., 1997. Multiple enrichment of the Carpathian-Pannonian mantle: Pb–Sr–Nd isotope and trace element constraints. J. Geophys. Res. 102 (B7), 14947–14961.
Roy-Barman, M., Wasserburg, G.J., Papanastassiou, D.A., Chaussidon, M., 1998. Osmim isotopic compositions and Re–Os concentrations in sulfide globules form basaltic glasses. Earth. Planet. Sci. Lett. 154, 331–347.
Rudnick, R.L., Goldstein, S.L., 1990. The Pb isotopic compositions of lower crustal xenoliths and the evolution of lower crustal Pb. Earth. Planet. Sci. Lett. 98, 192–207.
Saal, A.E., Hart, S.R., Shimizu, N., Hauri, E.H., Layne, G.D., 1998. Pb isotopic variability in melt inclusions from oceanic island basalts, Polynesia. Science 282, 1481–1484.
Salters, V.J.M., Mallick, S., Hart, S.R., Langmuir, C.H., Stracke, A., 2011. Domains of depleted mantle: new evidence from hafnium and neodymium isotopes. Geochem. Geophys. Geosyst. 12 (8), Q08001.
Salters, V.J.M., Stracke, A., 2004. Composition of the depleted mantle. Geochem. Geophys. Geosyst. 5(5).
Seyler, M., Bonatti, E., 1997. Regional-scale melt-rock interaction in lherzolitic mantle in the Romanche Fracture Zone (Atlantic Ocean). Earth. Planet. Sci. Lett. 146, 273–287.
Seyler, M., Cannat, M., Mével, C., 2003. Evidence for major-element heterogeneity in the mantle source of abyssal peridotites from the Southwest Indian Ridge (52° to 68°e). Geochem. Geophys. Geosyst. 4 (2), 10.
Seyler, M., Lorand, J.-P., Dick, H.J.B., Drouin, M., 2007. Pervasive melt percolation reactions in ultra-depleted refractory harzburgites at the Mid-Atlantic Ridge, 15°20′N: ODP Hole 1274A. Contrib. Mineral. Petrol. 153, 303–319.
Seyler, M., Toplis, M.J., Lorand, J.-P., Luguet, A., Cannat, M., 2001. Clinopyroxene microtextures reveal incompletely extracted melts in abyssal peridotites. Geology 29 (2), 155–158.
Shimazaki, H., MacLean, W.H., 1976. An experimental study on the partition of zinc and lead between silicate and sulfide liquids. Mineralium Deposita 11, 125–132.
Shirey, S.B., Bender, J.F., Langmuir, C.H., 1987. Three-component isotopic heterogeneity near the Oceanographer transform, Mid-Atlantic Ridge. Nature 325, 217–223.
Shirey, S.B., Richardson, S.H., 2011. Start of the Wilson cycle at 3 Ga shown by diamonds from subcontinental mantle. Science 333, 434–436.
Shirey, S.B., Walker, R.J., 1998. The Re–Os isotope system in cosmochemistry and high-temperature geochemistry. Ann. Rev. Earth Planet. Sci. 26, 423–500.
Sims, K.W.W., DePaolo, D.J., 1997. Inferences about mantle magma sources from incompatible element concentration ratios in oceanic basalts. Geochim. Cosmochim. Acta 61 (4), 765–784.
Sleep, N.H., Barth, G.A., 1997. The nature of oceanic lower crust and shallow mantle emplaced at low spreading rates. Tectonophysics 279, 181–191.
Snow, J.E., Reisberg, L., 1995. Os isotopic systematics of the morb mantle: results form altered abyssal peridotites. Earth. Planet. Sci. Lett. 136, 723–733.
Standish, J.J., 2006. The influence of ridge geometry at the ultraslow-spreading Southwest Indian Ridge (9°-25°E): basalt composition sensitivity to variations in source and process. Ph.D. Thesis, MIT/WHOI Joint Program.
Standish, J.J., Dick, H.J.B., Michael, P.J., Melson, W.G., O'Hearn, T., 2008. MORB generation beneath the ultraslow spreading Southwest Indian Ridge (9–25°E): major element chemistry and the importance of process versus source. Geochem. Geophys. Geosyst. 9 (5).
Stracke, A., Snow, J.E., Hellebrand, E., von der Handt, A., Bourdon, B., Birbaum, K., Günther, D., 2011. Abyssal peridotite Hf isotopes identify extreme mantle depletion. Earth. Planet. Sci. Lett. 308, 359–368.
Sun, S.-s., 1980. Lead isotopic study of young volcanic rocks from mid-ocean ridges, ocean islands and island arcs. Philos. Trans. Roy. Soc. Lon. A 297, 409–445.
Sun, S.S., Hanson, G.N., 1975. Evolution of the mantle: geochemical evidence from alkali basalt. Geology 3 (6), 297–302.
Tatsumoto, M., 1966. Genetic relations of oceanic basalts as indicated by lead isotopes. Science 153, 1094–1101.
Todt, W., Cliff, R.A., Hanser, A., Hofmann, A.W., 1996. Evaluation of a ^{202}Pb–^{205}Pb double spike for high-precision lead isotope analysis. In: Basu, A., Hart, S. (Eds.), Earth Processes: Reading the Isotopic Code. Geophysical Monograph, vol. 95. American Geophysical Union, pp. 429–437.
Warren, J.M., Shimizu, N., 2010. Cryptic variations in abyssal peridotite composition: evidence for recent melt-rock reaction at the ridge. J. Petrol. 51, 395–423.
Warren, J.M., Shimizu, N., Sakaguchi, C., Dick, H.J.B., Nakamura, E., 2009. An assessment of upper mantle heterogeneity based on abyssal peridotite isotopic compositions. J. Geophys. Res. 114 (B12203).
Widom, E., Hoernle, K.A., Shirey, S.B., Schmincke, H.U., 1999. Os isotope systematics in the Canary Islands and Madeira: Lithospheric contamination and mantle plume signatures. J. Petrol. 40 (2), 279–296.
Witt-Eickschen, G., Seck, H.A., Mezger, K., Eggins, S.M., Altherr, R., 2003. Lithospheric mantle evolution beneath the Eifel (Germany): Constraints from Sr–Nd–Pb isotopes and trace element abundances in spinel peridotite and pyroxenite xenoliths. J. Petrol. 44 (6), 1077–1095.
Workman, R.K., Hart, S.R., 2005. Major and trace element composition of the depleted MORB mantle (DMM). Earth. Planet. Sci. Lett. 231, 53–72.
Yao, H.-Q., Zhou, H.-Y., Peng, X.-T., Bao, S.-X., Wu, Z.-J., Li, J.-T., Sun, Z.-L., Chen, Z.-Q., Li, J.-W., Chen, G.-Q., 2009. Metal sources of black smoker chimneys, Endeavour Segment, Juan de Fuca Ridge: Pb isotope constraints. Appl. Geochem. 24, 1971–1977.
York, D., 1966. Least-squares fitting of a straight line. Can. J. Phys. 44, 1079–1086.
Zangana, N.A., Downes, H., Thirlwall, M.F., Hegner, E., 1997. Relationship between deformation, equilibration temperatures, REE and radiogenic isotopes in mantle xenoliths (Ray Pic, Massif Central, France): an example of plume-lithosphere interaction. Contrib. Mineral. Petrol. 127, 187–203.
Zindler, A., Hart, S., 1986. Chemical geodynamics. Ann. Rev. Earth Planet. Sci. 14, 493–571.
Zindler, A., Jagoutz, E., Goldstein, S.L., 1982. Nd, Sr and Pb isotopic systematics in a three-component mantle: a new perspective. Nature 298, 519–523.